PROCESS OF CREATING A MORE EFFICIENT REAL-TIME QUANTITATIVE PCR ASSAY TO DETECT *ANAPLASMA PHAGOCYTOPHILUM, BABESIA MICROTI, BORRELIA BURGDORFERI,* AND *BORRELIA MIYAMOTOI* THAT INHABIT DEER TICKS

by

RACHAEL ALLAN

A thesis submitted to the

School of Graduate Studies

Rutgers, The State University of New Jersey

In partial fulfillment of the requirements

For the degree of

Master of Science

Graduate Program in Microbial Biology

Written under the direction of

Alvaro Toledo

And approved by

_____

_____

_____

New Brunswick, New Jersey

May, 2019

ABSTRACT OF THE THESIS

PROCESS OF CREATING A MORE EFFICIENT REAL-TIME QUANTITATIVE PCR ASSAY TO DETECT *ANAPLASMA PHAGOCYTOPHILUM, BABESIA MICROTI, BORRELIA BURGDORFERI*, AND *BORRELIA MIYAMOTOI* THAT INHABIT DEER TICKS

By RACHAEL ALLAN

Thesis Director:

Alvaro Toledo

Ixodes scapularis, the most abundant tick species in New Jersey, is a vector for a host of human diseases, including Lyme disease, Anaplasmosis, Babesiosis, and *B. miyamotoi*. The prevalence of these diseases continues to steadily increase, and it has become critical to develop molecular methods to detect them. This project focuses on transitioning from a standard PCR and gel electrophoresis methodology to real-time PCR to screen for four common pathogens found in deer ticks – *B. burgdorferi, B. miyamotoi, A. phagocytophilum,* and *B. microti*. Primers and probes were created to target genes that were unique to each pathogen. They were tested using standard PCR and gel electrophoresis and were then optimized with real-time PCR using SYBR Green and TaqMan methodologies. The primer specificity was also assessed using tick DNA as a template utilizing a SYBR Green methodology. 158 deer ticks were tested for the presence of pathogens – 11.39% of deer ticks tested positive for *B. burgdorferi*, 6.33%

tested positive for *B. microti*, 6.96% tested positive for *B. miyamotoi*, and 10.76% tested positive for *A. phagocytophilum*. With all of these steps completed, a multiplex PCR assay can be created to screen for all four pathogens in one single test tube.

ACKNOWLEDGEMENTS

I would like to thank everyone who has believed and guided me throughout my research.

New Jersey Laboratories – To owner Michael Rockoff, thank you for funding my research and for giving me the opportunity to improve our tick testing service. To the CEO, Sandra Lee, thank you for letting me conduct my research and for all of your support. To QA and Regulatory Affairs Manager, Soumya Nanda, thank you for your unwavering support, love, and guidance throughout the duration of this project. You have been my driving force and inspiration to never give up on my dreams and to always believe in myself. To Microbiology Lab Manager, John Jaglowski, thank you for your help with ordering materials for my research. To Microbiologist, Craig Spitzmiller, thank you for all of your support, pep talks, and for taking me under your tick-testing wing. To Research Scientist, Rachel Brick, thank you for answering all my research questions and for sharing your knowledge and expertise with research. To Microbiology Technician, Margarita Carrasco, thank you for helping me learn how to make proper LB media for my agar plates and broth cultures. To everyone else at New Jersey Laboratories, thank you for making me feel so welcomed and always a part of the family.

Rutgers University – To Academic Advisor, Gerben Zylstra, thank you for providing me with the opportunity to conduct my thesis through New Jersey Laboratories and for your advice throughout the duration of this project. To Research Advisor, Alvaro Toledo, thank you for your help with the design of the project and for bringing my ideas to life. To Quality Assurance Management Professor, Sheila Lawrence, thank you for helping me

analyze my work from a quality standpoint, as well as your support with my cost-benefit analysis.

Home – To my parents Rena and Scott Allan and my brother Eric, thank you for believing in me and for helping me accomplish my dreams. To my loving boyfriend, Brian Van Oostendorp, thank you for being my rock, for always supporting me, and for helping me believe in myself. To Taylor Moore, thank you for all of your positive advice, love, and support when I needed it the most. To my sweet dog, Skyy, thank you for all of your dog snuggles, face licks, and play time in between my work. Thank you to the rest of my extended family and friends for sticking by my side throughout my graduate school journey.

TABLE OF CONTENTS

LIST OF TABLES

LIST OF FIGURES

INTRODUCTION

IXODES SCAPULARIS

Ixodes scapularis, more commonly known as the black-legged tick or the deer tick, is a blood sucking arthropod and the vector of a plethora of human diseases, including Lyme disease, Human Granulocytic Anaplasmosis (HGA) and human babesiosis among others (1, 2). Taxonomically, *I. scapularis* ticks belong to the subclass *Acari*, which includes mites and ticks. One of the main characteristics of ticks is that they have a reduced body segmentation. The prosoma and opitosoma are fused to form the idiosoma or body, which includes organs and functions associated with the head, thorax, and abdomen in insects. On the other hand, the mouth and feeding parts are separated from the body and constitute the gnanothosoma (1, 2). In ticks, the first and second pair of appendages are modified to form the chelicera and pedipalps, which cover the hypostome. The chelicera are pincher-like claws that pierce the skin and facilitate the introduction of the hypostome, a harpoon-like structure that allows ticks to attach to a host during feeding (1, 2).

The genus *Ixodes* have a broad geographic distribution range, including America, Asia, and Europe (3). In the United States, *Ixodes scapularis* and *Ixodes pacificus* are found on the east and west cost of the USA respectively while a third nidicolous species, *Ixodes cookie*, is associated with the woodchuck. In New Jersey, *Ixodes scapularis* is the most abundant tick species. Typically, *I. scapularis* can be found along the eastern seaboard of the United States and the upper Midwest where moist weather conditions occur year-round and mild temperatures persist through the winter months. Since *I. scapularis* vectors several pathogens whose prevalence has steadily increased over the

last two decades, it has become critical to develop molecular methods to detect these pathogens in the tick in a cost-effective manner.

IXODES SCAPULARIS - LIFE CYCLE AND FEEDING STAGES

Ixodes scapularis has four different stages (Figure 1) – egg, larva, nymph, and adult – in a two year life cycle (4). Ticks are opportunistic ectoparasites that feed on a wide range of hosts. Nonetheless, three-host tick species, such as *I. scapularis* have preferred hosts for each tick stage. In general, larvae and nymphs feed on small animals, mostly rodents and occasionally lizards and birds while adult ticks feed on larger animals including the white-tailed deer, the most common host, as well as foxes, black bears, and raccoons (4).

Ixodes scapularis has a two-year life cycle (Figure 1). Eggs hatch into larvae during the summer months and start questing for a host, typically small rodents such as the white-footed mice. Larvae feed only once and they uptake blood until they are fully engorged. At this point, the tick is ready to drop off and molt into a nymph (4). Nymphs will enter diapause and spend the winter in a dormant stage until the following spring. Environmental cues including temperature, as well as daylight, activate nymphs in the early spring (4). Nymphs feed on medium-sized mammals, uptake blood until they are fully engorged, and then drop off and molt into an adult (5).In the fall, adult ticks feed and mate on a large host, typically a deer. Engorged female ticks drop off and lay around 3,000 eggs before dying (4).

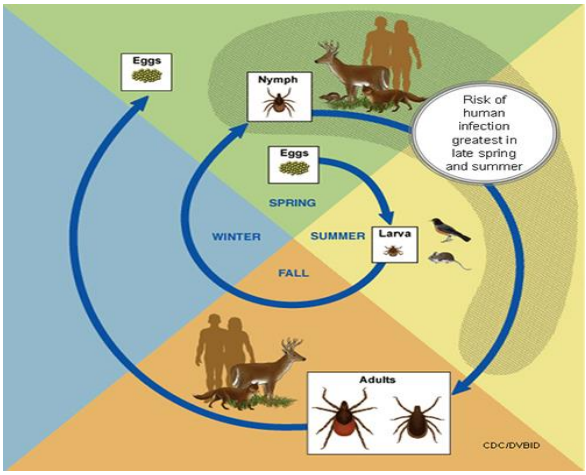

Figure 1: Life cycle of *Ixodes scapularis* (4).

IXODES SCAPULARIS – FEEDING AND TRANSMISSION OF TICK-BORNE DISEASES

Deer ticks quest by climbing the vegetation (leaves, tall grass, and shrubs) where they ambush the host. Ticks hold onto the vegetation with their 2 to 4 posterior pair of legs while they extend and move the first pair of legs to latch onto an incoming vertebrate host (4, 5). The tick questing behavior depends on environmental factors, including temperature and humidity. Ticks recognize a host by detecting movement and carbon dioxide. These host cues increase the questing activity of the tick and facilitate host-seeking success. On the host, deer ticks will cut through the surface of the host's skin with the chelicera and insert the hypostome into the host's skin to start feeding (6). The tick injects saliva, which contains anesthetics and anticoagulants, into the host to facilitate feeding (4). The length of the feeding process depends on the stage of the tick and takes between three and twelve days (4, 5).

I. scapularis ticks acquire pathogens while feeding on an infected host. Once a tick is infected, it remains infected throughout its life cycle. This is known as transstadial

transmission. On the other hand, the transmission of pathogens from adults to the next generation (larvae) is known as transovarial transmission. Pathogens transmitted by *I. scapularis* do not have transovarial transmission (with the exceptions of RF *Borrelia* and Powassan virus). Thus, larvae are not infected and do not play a role in the transmission of diseases (7, 8).

Since nymphs are active during the spring, humans are more likely to encounter them during outdoor activities, such as hiking or camping (4, 5, 7). Nymphs are very small (1-1.5 mm) and hard to notice. Removal of ticks in a timely fashion decreases the chances of pathogen transmission (5). Adults, which are active throughout the fall, can also transmit diseases, but compared to nymphs, they are easier to spot and remove before pathogen transmission occurs (7, 8).

TICK-BORNE DISEASE DISTRIBUTION

There are four common tick-borne bacterial pathogens that are found in deer ticks – *Anaplasma phagocytophilum, Babesia microti, Borrelia burgdorferi,* and *Borrelia miyamotoi.* The geographic distribution of *Ixodes scapularis* (Figure 2), includes the northeastern region of the United States along with the Midwest and the South.

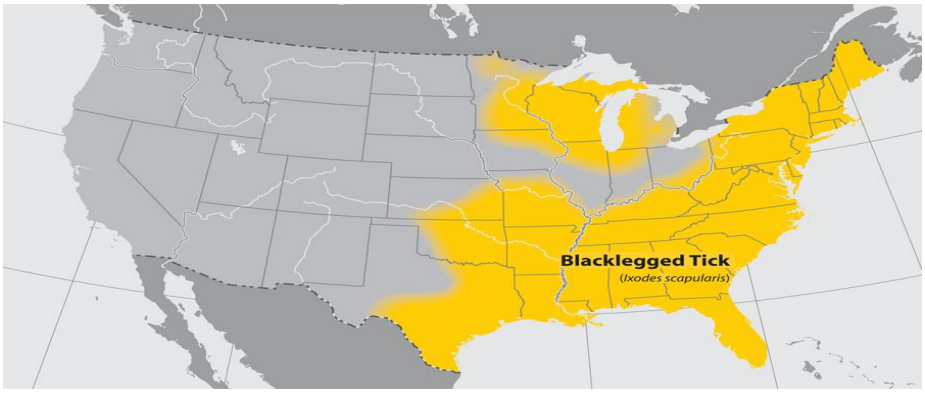

Figure 2: Geographic distribution of *Ixodes scapularis* – deer ticks (9).

ANAPLASMA PHAGOCYTOPHILUM - OVERVIEW

History

The first reference to *A. phagocytophilum* dates back to 1932 when a tick-borne agent was thought to produce a febrile illness in sheep in Scotland (10). In 1951, the bacterium was found in the granulocytes of neutrophils and was classified as a *Rickettsia* (11). In 1962, the microbe was moved into the genus *Ehrlichia* after taxonomic reclassification (11, 12). In 1994, the agent was isolated from patients from Minnesota and Wisconsin that were bitten by deer ticks and that had developed symptoms of anaplasmosis (13, 14). It was at this time that *Ehrlichia phagocytophila* was named the causative agent of Human Granulocytic Ehrlichiosis (HGE). In 2001, after exhaustive genetic examination, *E. equi*, and *E. phagocytophila* were merged and reclassified as *Anaplasma phagocytophilum* (14-16).

Etiological Agent and Transmission

A. phagocytophilum is a Gram-negative intracellular bacterium with a small circular DNA (1500 kb) and a limited metabolic capacity. In the United States, *A. phagocytophilum* can be found in *Ixodes* ticks that act as vectors, as well as in mammalian hosts, including racoons, squirrels, white-footed mice, and deer (13-15). When the agent of HGA infects humans, it disseminates and reaches the spleen and bone marrow where it can infect and replicate in granulocytes, a type of white blood cell that contains granules (13-15). *Anaplasma* infected neutrophils do not function properly and they eventually burst releasing bacteria to the blood stream (16, 17).

Clinical Symptoms, Signs and Treatment

HGA has an incubation time of one to two weeks and initially causes a febrile illness with symptoms similar to the common cold, including fever, chills, muscle aches, and loss of appetite. A prompt diagnosis is critical since untreated patients can develop more serious complications including respiratory failure, renal failure, coma, seizures, and even death (14, 18). Nonetheless, HGA is treatable with doxycycline and when it is administered early during the infection, potential complications can be prevented (19).

Incidence

The cases of HGA (Figure 3) are concentrated in the northeast and Upper Midwest of the USA. According to a report from the CDC from 2016, the CDC noted that the number of cases of HGA could range from 3 to 26 per one million of people in New Jersey alone and that the highest number of cases were found in New York, Rhode Island, New Hampshire, Massachusetts, Vermont, Minnesota, and Wisconsin (19). The map in Figure 3 indicates the rate of new cases of the disease in 2016. The expansion of the vector to new areas may facilitate the continuous emergence of this bacterium throughout the US.

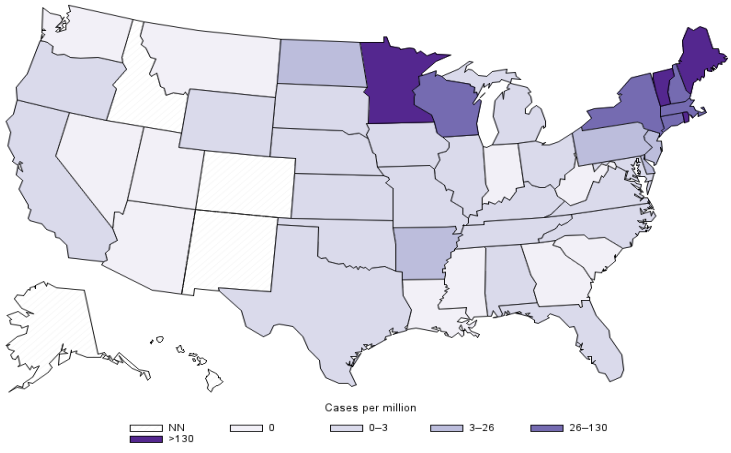

Figure 3: Cases per Million of People with Anaplasmosis in 2016 (19).

BABESIA MICROTI – OVERVIEW

History

The first human case of babesiosis was reported in Croatia in 1957 on a cattle farm. The farmer was splenectomized and had become infected with the disease after getting bitten by one of the many deer ticks found on the farm. He ended up succumbing to the disease. In the United States, the first human case of babesiosis transmitted by *I. scapularis* was reported in 1979. A woman from Nantucket Island, Massachusetts, was diagnosed with the disease by doctors in New Brunswick, New Jersey (20-22).

Etiological Agent and Transmission

There are several species of *Babesia* that cause Human babesiosis. Nonetheless, in the United States, the only *Babesia* species that affects humans is *B. microti*. Unlike the other pathogens included in this study, *B. microti* is a protozoan parasite that belongs to the phylum apicomplexan, which is characterized by having an apical complex critical for motility, adhesion and invasion of host cells. *Babesia* are often referred as piroplasms due to their characteristic pyriform or pear shape within erythrocytes where they reproduce by merogony. Interestingly, *Babesia* species have a quite complex life cycle that involves tick vectors where they reproduce sexually and mammalian hosts where they reproduce asexually (22, 23).

The transmission of *B. microti* (Figure 4) is transstadial where the infection of the pathogen continues from one stage of life to the next (24). The life cycle of *Babesia microti* is complex as the protozoan needs two hosts – a tick and a rodent – and must go through sexual and asexual reproduction (25). Typically, transmission begins with an

infected *Ixodes scapularis* tick feeding on a white-footed mouse or other small rodent. In the rodent, the sporozoites enter red blood cells where asexual reproduction takes place. When an uninfected tick feeds on the infected rodent, it digests the gametes that have formed in the rodent during asexual replication. The gametes inside of the newly infected tick then get fertilized and form sporozoites during sexual replication. When the tick with the sporozoites feeds on a human host, the sporozoites enter red blood cells where asexual reproduction and replication happens and thus results in human babesiosis. Since *Babesia microti* is found in the red blood cells, and can be transferred in blood transfusions, it is important to recognize its presence to prevent further spreading of the disease (25).

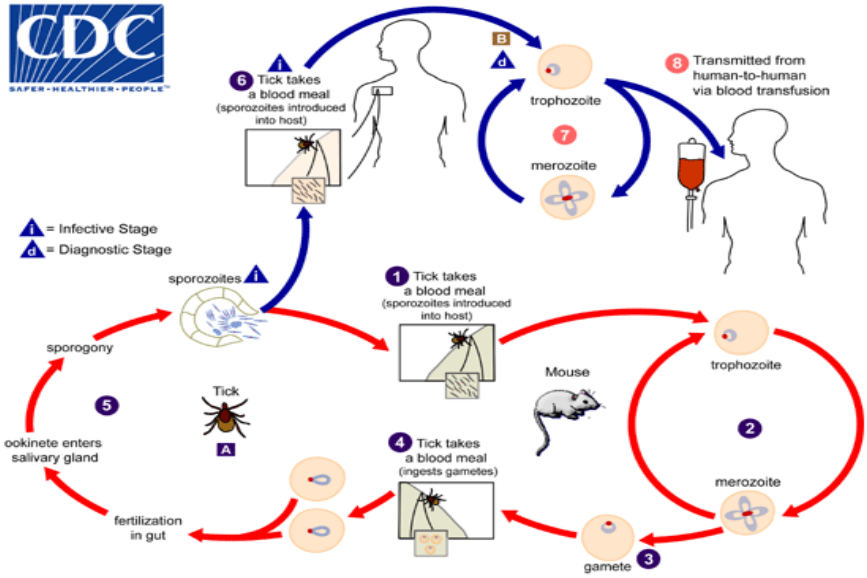

Figure 4: Life cycle of *Babesia microti* (25).

Clinical Symptoms, Signs, and Treatment

Splenectomized or immunodepressed patients, especially those over the age of 50, can become sick with babesiosis. In healthy individuals, however, the disease is subclinical. Symptoms include flu-like symptoms, such as fever, headache, nausea, and

chills that might become present one to six weeks after a tick's bite (26). If left untreated or misdiagnosed, the disease can lead to further complications, including anemia, low blood pressure, and organ failure, or even death (27-29). For treatment, two prescription medications are utilized at the same time to combat the disease – either atovaquone and azithromycin or clindamycin and quinine (28). These treatments are effective in preventing the disease from becoming deadly.

Incidence

The incidence of *B. microti* includes the Northeast and upper Midwest of the United States with a concentration of the microbe found in New Jersey, New York, Minnesota, and Wisconsin (29). Most cases of babesiosis (Figure 5) are reported by people over 50 years old that live in endemic areas during the warmer months of the year (28, 29).

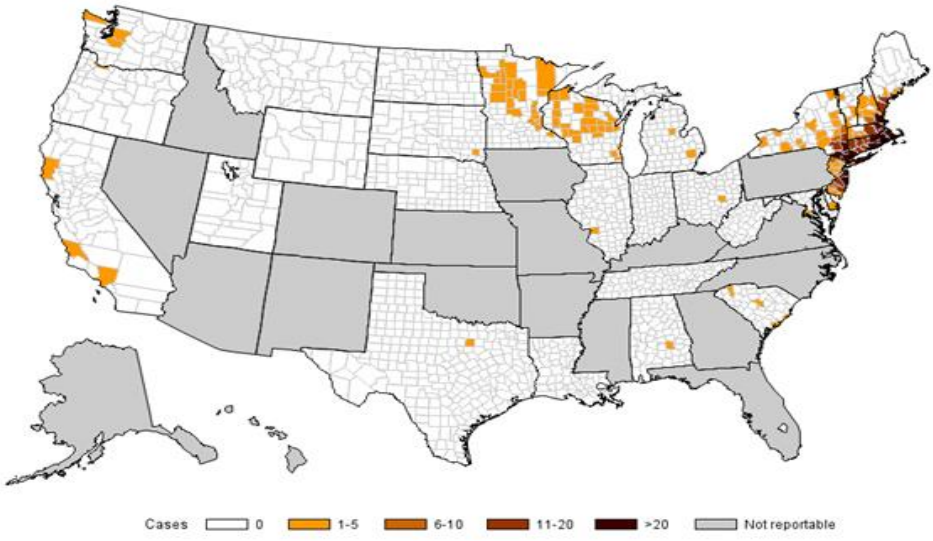

Figure 5: Cases of Babesiosis by county in 2014 (29).

BORRELIA BURGDORFERI – OVERVIEW

History

The spirochete was first discovered after the Connecticut Health Department launched an investigation on an outbreak of juvenile arthritis in Old Lyme (30). The initial investigation concluded that patients that developed arthritis in major joints lived near wooded areas and often developed a skin lesion before the onset of arthritis, suggesting that arthritis was a clinical manifestation of an infectious disease. The spirochete was first isolated from the midguts of deer ticks collected from Shelter Island, New York, and was recognized by sera from patients diagnosed with Lyme disease (30, 31).

Etiological Agent and Transmission

The diderm, flat-waved spirochete, *B. burgdorferi*, is the causative agent of Lyme disease. *Borrelia burgdorferi* is maintained in sylvatic cycles between the deer tick and small rodents (32-34). When an infected tick feeds on a human, the spirochete migrates from the midgut to the salivary glands and subsequently enters the human host (32). To survive in mammalian hosts, *Borrelia burgdorferi* adapts to the changing host environments by varying its gene expression (35).

B. burgdorferi has a small, metabolic-limited genome and depends on the mammalian host to obtain nutrients to grow and multiply (35). With the use of its endoflagella, *B. burgdorferi* can swim towards nutrients and away from toxins even in a viscous environment (36). As the endoflagellum rotate, *Borrelia burgdorferi* can alter its morphology and become planar to move more effectively through viscous media.

Furthermore, motility is such an important trait that the spirochete devotes 6% of its genome to motility-related genes.

Clinical Symptoms, Signs, and Treatment

Symptoms and signs of Lyme disease progress over time and become more dangerous the longer the spirochete is left untreated. In the first couple days to one month, symptoms are similar to the common cold along with muscle pain, aching joints, and swollen lymph nodes. An Erythema migrans or "bull's eye" rash occurs in 70-80% of people infected with Lyme disease. The rash begins at the location of the tick bite and then spreads to other parts of the body. If Lyme disease is left untreated for months, more serious complications can accrue, including arthritis, neck stiffness, heart palpitations, nerve damage, brain and spinal cord inflammation, facial palsy, and shooting pain throughout the body (30, 37, 38). Lyme disease is treatable with an appropriate course of doxycycline.

Incidence

Furthermore, the incidence of *B. burgdorferi* (Figure 6) encompasses the northeastern states and the upper Midwest. In 2016, the CDC noted that Lyme disease was most common in New Jersey, New York, Delaware, Pennsylvania, and other neighboring states and that approximately 30,000 cases are reported each year. However, it is suggested that the cases not reported to the CDC can be more than 10-fold higher with over 300,000 people becoming infected with the Lyme disease spirochete every year. Just

as the deer ticks become more widespread, the cases of Lyme disease continue to increase from year to year (38).

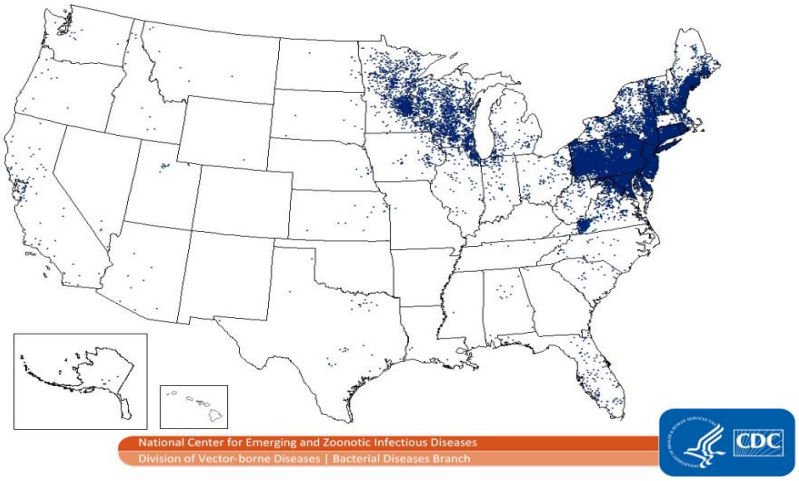

Figure 6: Individual Cases of People with Lyme disease in 2016 (38).

BORRELIA MIYAMOTOI **– OVERVIEW**

History

Gram-negative, spiral-shaped bacterium, *Borrelia miyamotoi*, was discovered in Japan in 1995 by Kenji Miyamoto (39, 40). The spirochete was isolated from the midgut of a deer tick from Hokkaido, Japan, and genetic analysis determined that it belonged to the relapsing fever *Borrelia* group (39, 40). In 2011, the first human cases of the disease were found in patients that lived in Russia (41).

Etiological Agent and Transmission

Borrelia miyamotoi is a spirochete from the genus *Borrelia*; however, it is more closely related to tick-borne relapsing fever *Borrelia* than to Lyme disease *Borrelia* (39). *B. miyamotoi* has a spiral shape that inhabits *Ixodes* tick vectors, which is unique for this

relapsing fever *Borreliae* since other species typically inhabit soft ticks. *B. miyamotoi* is transmitted transstadially and has an enzootic life cycle that includes the tick vectors, as well as vertebrate hosts (39). *B. miyamotoi* replicates in the bloodstream and its prevalence in humans is much lower than *B. burgdorferi* (39, 42).

Clinical Symptoms, Signs, and Transmission

Since *B. miyamotoi* is a relapsing fever *Borrelia*, symptoms include fever, headache, dizziness, chills, nausea, and fatigue. Unlike *B. burgdorferi*, rashes and joint pain are uncommon (43, 44). *B. miyamotoi* is treated with doxycycline (42).

Incidence

Borrelia miyamotoi can be found in the same geographic regions as *B. burgdorferi*, including the northeastern states and the upper Midwest (42, 44). However, its incidence is much less than the incidence of *B. burgdorferi* (39, 42). The CDC notes that there are less than sixty documented cases of *B. miyamotoi* human infections in the United States (42).

IMPORTANCE OF TESTING THESE TICK-BORNE PATHOGENS

Due to a continuous emergence of tick-borne diseases in the USA, there is a need for fast, cost-effective tests to detect pathogens in the tick vector (45). Testing ticks can be used as an alternative for early diagnosis since the onset of tick-borne diseases is generally unspecific and cause a febrile illness (46). Despite that, in general, it is assumed that a tick needs to feed between 36-48 hours to efficiently transmit a bacterial or protozoan pathogen to a new host, there are instances in which this transmission can

occur earlier. In addition, estimating the feeding time can be tricky if the tick is not found right away. Serological diagnosis in human patients cannot be performed in the first two weeks after infection due to the lack of a detectable antibody response. Also, molecular methods have a low sensitivity for the Lyme disease spirochete, which is the most prominent tick-borne disease in the USA with an estimation of 300,000 cases per year (1). Furthermore, symptoms for these tick-borne diseases can vary, which can lead to doctors misdiagnosing patients (47). By testing the tick for tick-borne pathogens, doctors can address whether treatment is necessary (48). Lastly, most tick-borne disease diagnostic tests only target individual pathogens. Simultaneous detection of several pathogens through one screen can shorten the time for diagnosis, as well as address the potential for co-infections (46, 49).

HYPOTHESIS STATEMENT

Our hypothesis is that with quantitative PCR, we can develop an efficient methodology to simultaneously detect *Anaplasma phagocytophilum*, *Babesia microti*, *Borrelia burgdorferi*, and *Borrelia miyamotoi* in *Ixodes scapularis*. This new real-time PCR will replace the original PCR and gel electrophoresis methodology utilized in a company setting to test client deer ticks for the presence or absence of these tick-borne pathogens.

MATERIAL AND METHODS

GENERAL APPROACH

The deer tick, *I. scapularis*, is arguably the most abundant tick species in New Jersey and is commonly sent to the laboratory for pathogen testing. The deer tick is a competent vector for several human pathogens including *A. phagocytophilum*, *B. microti*, *B. burgdorferi*, and *B. miyamotoi*. Therefore, we decided to develop a multiplex real time PCR that would allow the simultaneous detection of all of these pathogens.

GENE SELECTION FOR PATHOGEN DETECTION

The criteria to select genes suitable for identifying *A. phagocytophilum, B. microti, B. burgdorferi*, and *B. miyamotoi*, were a) genes had to be unique to each human pathogen and b) had to be heterogeneous. This was to ensure that the pathogens were targeted by genes that would always be present in its genome.

ANAPLASMA PHAGOCYTOPHILUM – msp2 GENE

For *A. phagocytophilum*, the single-copy gene, *msp2* that encodes a major outer membrane surface protein, was chosen as the target for the quantitative PCR (50). The Msp-2 protein is an adhesin that facilitates infection of granulocytes and plays an important role in adhesion to cell surfaces (51). This gene is not found in the *Ehrlichia* family, except for *A. marginale*, which is not endemic to New Jersey (52). The *msp2* gene is part of the OMP-1/MSP2/P44 protein family, which is thought to help the microbe to survive in different environmental conditions, as well as in different hosts (50). This gene

has been used in real-time PCR, both singleplex and multiplex reactions, previously to identify *A. phagocytophilum* in deer ticks (50, 53).

BABESIA MICROTI – 18S rRNA GENE

For *B. microti*, the 18S rRNA gene was chosen as the target for quantitative PCR. This gene is conserved in all strains of *Babesia microti* in the United States (54). The 18S rRNA is present in eukaryotes, like the protozoan parasite *B. microti*, but are absent in prokaryotes (54). Thus, primers and probes needed to be specific to ensure that they detect *Babesia microti* and do not cross react to *I. scapularis*.

BORRELIA BURGDORFERI – ospA GENE

For *B. burgdorferi*, the outer surface protein A (*ospA*), which encodes a highly abundant outer membrane protein, is associated with survival in the tick vector (55). This gene is common across all strains of *B. burgdorferi* in the United States and is not found in *B. miyamotoi*, the other *Borrelia* species included in this study (48, 56). The *ospA* gene has been used at New Jersey Laboratories to screen for the presence of *B. burgdorferi* in ticks. Originally, the screening was performed using a standard PCR and the results were visualized in a gel. Thus, we decided to include this gene as the target for *B. burgdorferi* in a real-time PCR platform.

BORRELIA MIYAMOTOI – glpQ GENE

For *B. miyamotoi*, the *glpQ* gene, which encodes the enzyme glycerophosphodiester phosphodiesterase, was chosen as the target for quantitative PCR.

This enzyme helps to salvage the glycerol portion of triglycerides and phospholipids when they are broken down as an energy source (57). The *glpQ* gene is present in all relapsing fever *Borrelia* species but is absent in Lyme disease *Borrelia* species and has been largely used to differentiate between both groups (57-59).

SELECTION OF INTIAL PRIMERS AND PROBES

Primer Express Software from Thermo Fisher Scientific was utilized to design primers and probes for the four genes mentioned above (Table 1). A first approach rendered a set of primers and probes there were not specific enough to multiplex all the pathogens targeted. Thus, we decided to use an alternative software, Beacon Designer™ from Premier Biosoft. This software helped us to design *in silico* primer and probe sets that were specific for each tick-borne pathogen (Table 2). Using the same software, a second set of primers and probes were designed (Table 3). When compared, the first set of primers and probes was superior and ultimately it was chosen to proceed for further optimization.

When designing the primers and probes using Beacon designer, multiplexing guidelines were followed. For the primers, the melting temperatures were similar to each other and the lengths ranged from 18 to 28 basepairs (60, 61). For the probes, the melting temperatures were around 10 °C higher than the melting temperature of the primers and the lengths ranged from 20 to 30 basepairs (60). This was to ensure that the probes would stay bound to the template DNA long enough for the primer extension step of the PCR to be conducted.

The free energy of the primer to primer interactions, as well as the primer to probe interactions had to be higher than -9 kcal/mole (60). Internal dimers higher than -6 kcal/mole and interactions with the 3' end of the primers and probes were higher than -5 kcal/mole. Finally, the primers and probes did not have more than three G or C bases in a row within the last five bases on the 3' end. With these guidelines taken into consideration, the most optimal primers and probes were chosen for the continuation of this project.

While optimizing the probes, different quenchers were used (Table 4). The original set of probes had QSY quenchers with the fluorescent dyes FAM and VIC; however, the probes did not bind to the template DNA. The QSY quenchers were replaced with MGB quenchers with the same fluorescent dyes (FAM and VIC).

Table 1: Initial set of primers and probes designed using Primer Express software from Thermo Fisher Scientific.

A. phagocytophilum (msp2)	Forward Primer	5'- GGCTTAGGTGTCGTTCCTTATGC -3'
	Reverse Primer	5'- ACAACGCCCACGAAGTTACC-3'
	Probe	5'- TGCGTCGGTCTTGG-3'
B. microti (18S rRNA)	Forward Primer	5'- CCCGACGGCCAAGGA-3'
	Reverse Primer	5'- TGCACGCGCGCTACAC-3'
	Probe	5'- AAACTCGTTGAATGCATC-3'
B. burgdorferi (ospA)	Forward Primer	5'- CCAAAGACAAGTCATCAACAGAAGAA-3'
	Reverse Primer	5'- GGTTCCGTCTGCTCTTGTTATTATTT-3'
	Probe	5'- AATGAAAAAGGTGAAGTATCTGA-3'
B. miyamotoi (glpQ)	Forward Primer	5'- TGTTATAATGCACGACCCAGAAA-3'
	Reverse Primer	5'- AGCTCGATTGGGAAATAATTGTG-3'
	Probe	5'- TGACACAACCACAAATG-3'

Table 2: Initial set of primers and probes designed using Beacon Designer software from Premier Biosoft.

A. phagocytophilum (msp2)	Forward Primer	5'- GCGTTGTTGTGGGCATATCAC-3'
	Reverse Primer	5'- CTCCCACAACACGATGGTAGAAA-3'
	Probe	5'- CTCTCTCCTGAAATCTCGGCTTT-3'
B. microti (18S rRNA)	Forward Primer	5'- CAAGGTGCTGAAGGAGTCGTTTA-3'
	Reverse Primer	5'- AGATACCGTCGTAGTCCTAACCA-3'
	Probe	5'- ACTGACGACCTCCAATCTCTAGT-3'
B. burgdorferi (ospA)	Forward Primer	5'- TCTGGAGTACTTGAAGGCGTAAA-3'
	Reverse Primer	5'- AAGTGTGGTTTGACCTAGATCGT-3'
	Probe	5'- AAAGTAAAGTAAAATTAACAATT-3'
B. miyamotoi (glpQ)	Forward Primer	5'- ACCATTGATCATAGCTCACAGGG-3'
	Reverse Primer	5'- AATCAGCTCCTAAGGCATAAGCA-3'
	Probe	5'- CCTTCCAGAACATACCTTAGAAG-3'

Table 3: Second set of primers and probes designed using Beacon Designer software from Premier Biosoft.

A. phagocytophilum (msp2)	Forward Primer	5'-GCTTGTTATGATCTTCTTAGTG-3'
	Reverse Primer	5'-AACCCAGCCTTTAATCTATAAG-3'
	Probe	5'-CCTTATGCTTGCGTCGGTCTT-3'
B. microti (18S rRNA)	Forward Primer	5'-CTCTGACAGTTAAATACGAATG-3'
	Reverse Primer	5'-GTAGGACTTTGGTTCTATTTTG-3'
	Probe	5'-CCAACTGCTCCTATTAACCATTACTCT-3'
B. burgdorferi (ospA)	Forward Primer	5'-GAACCAGACTTGAATACAC-3'
	Reverse Primer	5'-CCTTCTTTAACCACCAATG-3'
	Probe	5'-TCAGCAGTTAGAGTTCCTTCAAGAACA-3'
B. miyamotoi (glpQ)	Forward Primer	5'-GAAGGTATTGCTGAAGTTG-3'
	Reverse Primer	5'-GCATCTGTCCTAAATGTATAAG-3'
	Probe	5'-TGGAATTGGACCCTGGATACCC-3'

Table 4: Type of fluorogenic probes purchased to amplify the template DNA of each tick-borne pathogen.

Tick-Borne Pathogen	Trial 1	Trial 2
A. phagocytophilum (msp2)	QSY-VIC	Same as Previous – No Change
B. microti (18S rRNA)	QSY-FAM	Same as Previous – No Change
B. burgdorferi (ospA)	QSY-FAM	MBG-FAM
B. miyamotoi (glpQ)	QSY-VIC	MGB-VIC

PRIMERS, PROBES, AND PLASMID CONTROLS

Primers were resuspended in water to create a 100 μM stock solution. The stock solution was diluted further to 10 μM and 20 μM to use in the PCR reactions. The first set of probes (all with QSY quenchers) were diluted to 2 μM with Tris-EDTA buffer (10 mM Tris-HCl, 1 mM disodium EDTA, pH 8.0). The second set of probes (two MGB and two QSY) were diluted with TE buffer from Sigma-Aldrich (62). Positive control plasmids purchased from Thermo Fisher Scientific were resuspended in water to a final stock concentration of $5x10^9$ copies.

To calculate the copy number of each of the controls, the following equation (eq. 1) was utilized. It is important to note that X is the amount of ng of DNA, N is the length of the DNA sequence, and that 650 g/mole is the average mass of one basepair of the double stranded DNA.

$$\#\ copies = \frac{x(ng)\times 6.022\times 10^{23}\left(\frac{molecules}{mole}\right)}{N\times 650\ \left(\frac{g}{mole}\right)\times 1\times 10^{9}\left(\frac{ng}{g}\right)} \qquad \text{(eq. 1)}$$

NEGATIVE CONTROLS

The specificity of the primers was assessed using DNA from uninfected ticks purchased from the University of Oklahoma Tick Rearing Facility in Stillwater, Oklahoma. DNA was extracted from the ticks utilizing DNeasy Blood & Tissue Kit (Qiagen) and quantified. A total of 3 μL of tick DNA was used in each 20 μL PCR reaction tube.

POSITIVE CONTROLS

As positive controls, *B. burgdorferi* genomic DNA was purchased from the American Type Culture Collection. For *A. phagocytophilum*, *B. microti*, and *B. miyamotoi*, plasmids with the genes of interest inserted were used as positive controls. All plasmids were purchased from Thermo Fisher Scientific.

CREATION AND TRANSFORMATION OF POSITIVE CONTROL PLASMIDS

Positive control plasmids for *A. phagocytophilum*, *B. microti*, and *B. miyamotoi*, were purchased from GeneArt™ Plasmid Construction Service from Thermo Fisher Scientific. Each plasmid included the sequence of the targeted gene for one pathogen. Gene sequences obtained from GenBank were built into the GeneArt™ Plasmid Construction program. The plasmid maps for each of the constructs can be found below (Figures 7-9).

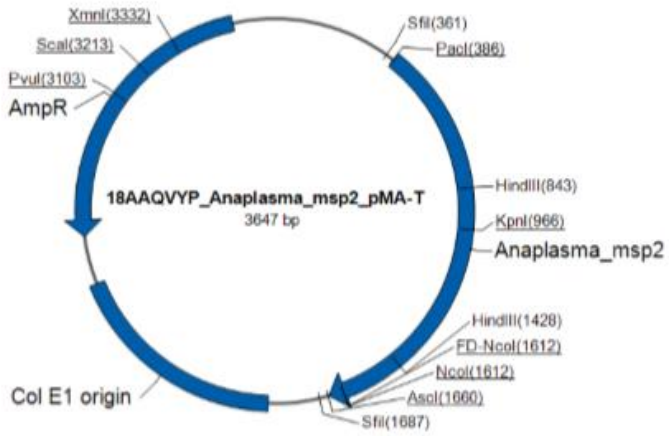

Figure 7: *A. phagocytophilum* plasmid (pMA-TANA) with the gene *msp2* inserted into the standard cloning vector pMA-T. The plasmid has an ampicillin resistance cassette.

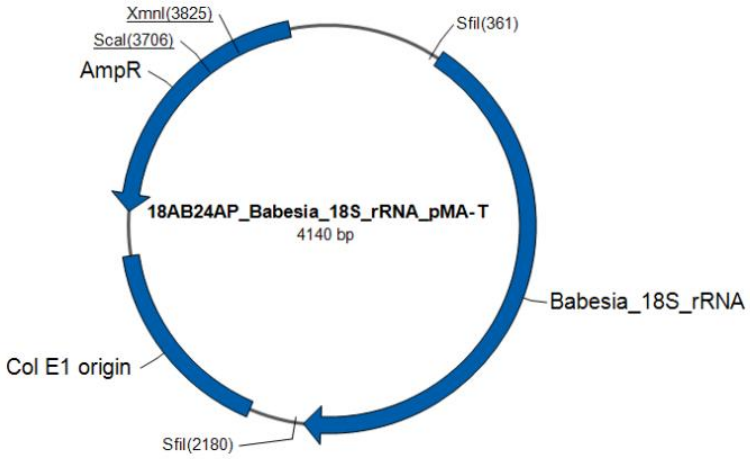

Figure 8: *B. microti* plasmid (pMA-TBAB) with the gene 18S rRNA inserted into the standard cloning vector pMA-T. The plasmid has an ampicillin resistance cassette.

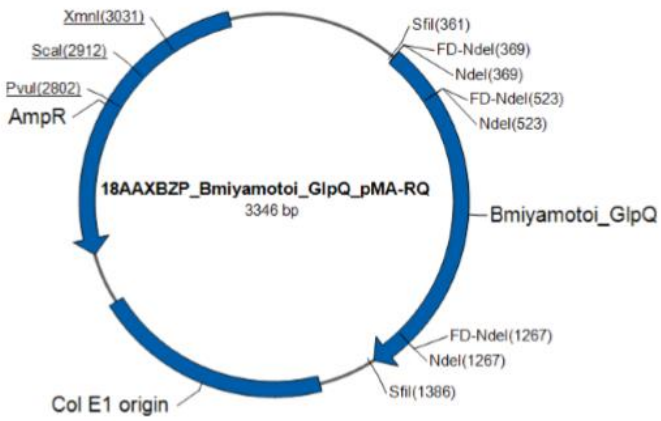

Figure 9: *B. miyamotoi* plasmid (pMA-RQMIY) with the gene *glpQ* inserted into the standard cloning vector pMA-RQ. The plasmid has an ampicillin resistance cassette.

The plasmids pMA-TANA, pMA-TBAB, and pMA-RQMIY were transformed in *E. coli* strain DH5α and clones selected in LB plates containing 100 μg/mL of ampicillin. Briefly, LB plates were made by adding 8.14 grams of Difco™ LB agar (Miller) to 220 mL of water. The mixture was heated and mixed on a hot plate (Thermo Fisher Scientific) until the LB agar powder was dissolved. A small aliquot of the liquid was poured into a small beaker to check the pH and the mixture was autoclaved.

A stock solution of 100 mg/mL of ampicillin (Teknova) was prepared by adding and vortexing 100 mg of ampicillin powder to 1 mL of distilled water. The ampicillin was filter sterilized using a 0.22-micron syringe filter and stored at 4 °C. Autoclaved LB agar was cooled down in a 45 °C water bath and 220 μL of the 100 μg/mL ampicillin was added. The agar was poured into sterile agar plates and stored at 4 °C.

Competent *E. coli* cells were thawed on ice while the agar plates were brought to room temperature. 3 μL of plasmid DNA (20 ng/μL) were added to 20 μL of competent cells in 2 mL centrifuge tubes. Tubes were gently mixed and incubated in ice for 30

minutes and brought up to 42 ℃ in a water bath (Thermo Fisher Scientific) for 45 seconds before getting placed back in ice for 2 minutes. Cells were plated on LB agar plates containing ampicillin and incubated overnight at 35 ℃. As a negative control, non-competent *E. coli* (ATCC® 8739™) was plated and incubated overnight at 35 ℃.

The following day, single colonies were picked and placed into Falcon tubes with LB broth with ampicillin and placed in a 37 ℃ shaking incubator (Fisher Scientific) for 17 hours. Plasmid DNA was quantified using a Qubit 3.0 Fluorometer (Thermo Fisher Scientific) and 1 μL of each aliquot of each plasmid was tested on the qPCR with SYBR Green primers at its quantified concentration.

OUTLINE OF PROJECT STEPS AND METHODS UTILIZED

1) Assess individual primers for each tick-borne pathogen.

   Method 1: Standard PCR followed by gel electrophoresis

   Method 2: Quantitative PCR using SYBR Green I

2) Optimize primer concentrations and annealing temperatures to maximize amplification efficiency for individual pathogens.

   Method 2: Quantitative PCR using SYBR Green I

3) Assess primer specificity using tick DNA as template.

   Method 2: Quantitative PCR using SYBR Green I

4) Switch real-time PCR from SYBR Green I to TaqMan and reassess sensitivity and specificity for each individual tick-borne pathogen.

   Method 3: Quantitative PCR using TaqMan

5) Optimize primer and probe concentrations, as well as annealing temperatures to maximize amplification efficiency for each individual pathogen.

   Method 3: Quantitative PCR using TaqMan

6) Combine optimized primers and probes to multiplex all tick-borne pathogens into one single reaction.

   Method 3: Quantitative PCR using TaqMan

PCR AND GEL ELECTROPHORESIS

Primers were tested at 0.50 μM, 1.00 μM, and 1.50 μM in each 50 μL PCR reaction. 1 μL of the positive controls at their stock concentrations ($5x10^9$ copies of the positive control plasmids and $5x10^6$ copies of. *B. burgdorferi* genomic DNA) was added. For the negative controls, water was added in place of the positive control DNA. The amplifications were carried out in a SimpliAmp Thermocycler (Thermo Fisher Scientific) (Table 5) following the master mix protocol (63). PCR products were ran on a 2% agarose gel and the results were stained and visualized with 1X BlueJuice™ Gel Loading Buffer (Thermo Fisher Scientific) and Safe Imager™ 2.0 Blue Light Transilluminator (Invitrogen).

Table 5: PCR run conditions using AmpliTaq Gold® 360 Master Mix (63).

Stage	**Step**	**Temperature, °C**	**Time**
Hold	Activate Master Mix	95	5 minutes
Cycles (30)	Denature	95	30 seconds
	Anneal	Primer Tm-5	30 seconds
	Extend	72	30 seconds
Hold	Extension	72	7 minutes
Hold	Hold	4	Infinite

SYBR GREEN I – PROCEDURE

Individual sets of primers were tested for the amplification of tick-borne pathogens by real-time PCR using 1X PowerUp™ SYBR™ Green Master Mix (Thermo Fisher Scientific) (64). Annealing temperatures and primer concentrations are displayed in Table 6.

Table 6: Reaction conditions for the first set of primers with PowerUp™ SYBR™ Green Master Mix.

Tick-Borne Pathogen	**Primer, µM**	**Annealing Temperature, °C**
B. burgdorferi genomic DNA (50,000-50 copies)	1.00	55
B. miyamotoi plasmid (pMA-RQMIY) (50,000-50 copies)	1.00	57
B. microti plasmid (pMA-TBAB) (50,000-50 copies)	1.00	56
A. phagocytophilum plasmid (pMA-TANA) (50,000-50 copies)	1.00	59

The following thermocycling conditions were used for DNA amplification (Table 7). A melt curve was performed to ensure that only one PCR product had been formed during the singleplex reactions.

Table 7: qPCR run conditions using PowerUp™ SYBR™ Green Master Mix (64).

Stage	**Step**	**Temperature, °C**	**Time**
Hold	UDG Activation	50	2 minutes
Hold	Dual-Lock™ DNA Polymerase	95	2 minutes
Cycles (40)	Denature	95	15 seconds
	Anneal	Primer Tm-5	15 seconds
	Extend	72	1 minute
Melt Curve	1.6°C/second	95	15 seconds
Melt Curve	1.6°C/second	60	1 minute
Melt Curve	0.15°C/second	95	15 seconds

A second set of primers were selected in an effort to increase efficiency. The optimization for this second set of primers was done using PowerUp™ SYBR™ Green Master Mix following the standard reaction conditions and protocol (64). Primer concentration, control DNA, as well as annealing temperature are shown in Table 8.

Table 8: Reaction conditions for the second set of primers with PowerUp™ SYBR™ Green Master Mix.

Tick-Borne Pathogen	**Primer, µM**	**Annealing Temperature, °C**
B. burgdorferi genomic DNA (50,000-50 copies)	1.00	45
B. miyamotoi plasmid (pMA-RQMIY) (50,000-50 copies)	1.00	46
B. microti plasmid (pMA-TBAB) (50,000-50 copies)	1.00	56
A. phagocytophilum plasmid (pMA-TANA) (50,000-50 copies)	1.00	54 55 56

TAQMAN - PROCEDURE

Two different master mixes were utilized to compare the PCR amplification results. First, TaqPath™ ProAmp™ Master Mix (Thermo Fisher Scientific) was utilized with the following cycle conditions (Table 9). When the amplification curves did not look clean, the master mix was switched to TaqMan™ Gene Expression Master Mix (Thermo Fisher Scientific), which was more equipped to amplify genes, and two different run methods were tried – the standard (Table 10) and fast (Table 11) (65, 66).

Table 9: qPCR run conditions using TaqPath™ ProAmp™ Master Mix (65).

Stage	Step	Temperature, °C	Time
Hold	First Denature and Enzyme Activation	95	10 minutes
Cycles (40)	Denature	95	15 seconds
	Anneal and Extend	Optimal Tm	60 seconds

Table 10: qPCR run conditions using TaqMan™ Gene Expression Master Mix Fast Method (66).

Stage	Step	Temperature, °C	Time
Hold	Uracil-N-Glycosylase Enzyme Incubation	50	2 minutes
Hold	DNA Polymerase Activation	95	2 minutes
Cycles (40)	Denature	95	1 second
	Anneal and Extend	Optimal Tm or 60	20 seconds

Table 11: qPCR run conditions using TaqMan™ Gene Expression Master Mix Standard Method (66).

Stage	Step	Temperature, °C	Time
Hold	Uracil-N-Glycosylase Enzyme Incubation	50	2 minutes
Hold	DNA Polymerase Activation	95	10 minutes
Cycles (40)	Denature	95	15 seconds
	Anneal and Extend	Optimal Tm or 60	1 minute

TAQMAN - FIRST SET OF PROBES

In each of the reactions with either the TaqPath™ ProAmp™ Master Mix or the TaqMan™ Gene Expression Master Mix, each 25 μL reaction included the 12.5 μL of 1X master mix, the optimized primer concentrations (1 μM), water, the probe (for either one of the two *Borrelias*), and genomic DNA/plasmid positive control copy number dilutions as presented in Tables 12-13.

Table 12: Reaction conditions for the first set of primers with TaqPath™ ProAmp™ Master Mix.

Tick-Borne Pathogen	**Primer, µM**	**Probe, nM**	**Annealing Temperature, °C**
B. burgdorferi genomic DNA (50,000-50 copies)	1.00	300 200 100 50	55
B. miyamotoi plasmid (pMA-RQMIY) (50,000-50 copies)	1.00	300 200 100 50	57

Table 13: Reaction conditions for the first set of primers with TaqMan™ Gene Expression Master Mix.

Tick-Borne Pathogen	**Primer, µM**	**Probe, nM**	**Annealing Temperature, °C**
B. burgdorferi genomic DNA (50,000-50 copies)	1.00	300 200	55
B. miyamotoi plasmid (pMA-RQMIY) (50,000-50 copies)	1.00	300 200	57

When both master mixes had little to no amplification of DNA, the copy numbers of the positive controls were increased while reverting to the TaqMan™ Gene Expression Master Mix with the Standard methodology. Fast cycling conditions of the TaqMan™ Gene Expression Master Mix with the normal 60 °C anneal and extend temperature was used.

As a last optimization attempt, a new strain of *Borrelia burgdorferi* genomic DNA was tried to see if the *Borrelia burgdorferi* probe would work with a different set of DNA. The TaqMan™ Gene Expression Master Mix was used with the Fast methodology with the annealing temperature step of 55 degrees Celsius. The *Borrelia burgdorferi* FAM QSY probe (300 and 200 nM) with the 1.00 μM optimized primers were used.

TAQMAN – SECOND SET OF PROBES

Since the two *Borrelia* probes did not work with any of the previously discussed master mixes, a second set of probes were tried with the TaqMan™ Gene Expression Master Mix (along with the probes for the other tick-borne pathogens) with the following primer and probe concentrations, as well as annealing temperature (Table 14).

Table 14: Reaction conditions for the second set of probes with TaqMan™ Gene Expression Master Mix.

Tick-Borne Pathogen	**Primer, µM**	**Probe, nM**	**Annealing Temperature °C**
B. burgdorferi genomic DNA (50,000-50 copies)	1.00	200 250 300	55
B. miyamotoi plasmid (pMA-RQMIY) (50,000-50 copies)	1.00	250	57
B. microti plasmid (pMA-TBAB) (50,000-50 copies)	1.00	250	55
A. phagocytophilum plasmid (pMA-TANA) (50,000-50 copies)	1.00 0.50 0.25	200 250 300	60

TAQMAN PRE-DESIGNED 18S rRNA EUKARYOTE ASSAY

A pre-designed 18S rRNA assay from Thermo Fisher Scientific was provided to see if the deer tick DNA, as well as genomic DNA of *Babesia microti*, could be amplified with the primers and probes provided with the assay. Since the probe and primers were supplied in a 20x vial, 1 µL of them along with 10 µL of the TaqMan™ Gene Expression Master Mix along with DNA and water were added into each PCR tube. For the PCR run

method, the conditions were used as provided from the TaqMan™ Gene Expression Master Mix Fast methodology (66).

RESULTS AND DISCUSSION

PART 1 – PRIMER AND PROBE SELECTION

1.1 RESULTS

After using the Premier Biosoft Beacon Designer software, it was imperative to verify that the sequences for the first and second sets of primers, as well as the probes, (Tables 2-4) were specific enough for each tick-borne pathogen. The primers and probes were analyzed as described in material and methods and there were no hits against any of the other pathogens included in the multiplex approach, as well as *Ixodes scapularis*.

1.2 TROUBLESHOOTING

The first set of primers and probes (Tables 2 and 4) were analyzed *in silico* using primer blast as described in material and methods and the results supported that they were specific for each target. In contrast, the second set of primers and probes of *B. miyamotoi* (Tables 3 and 4) showed unspecific binding to different genome regions of *A. phagocytophilum* (15 bp), *B. microti* (14 bp), and *I. scapularis* (14 bp) when analyzed *in silico* with primer blast (Figure 10). The unspecific binding of primers to DNA affects dramatically the sensitivity and performance of the PCR. Nonetheless, before discarding the primers, we looked closer to the hits found through primer blast.

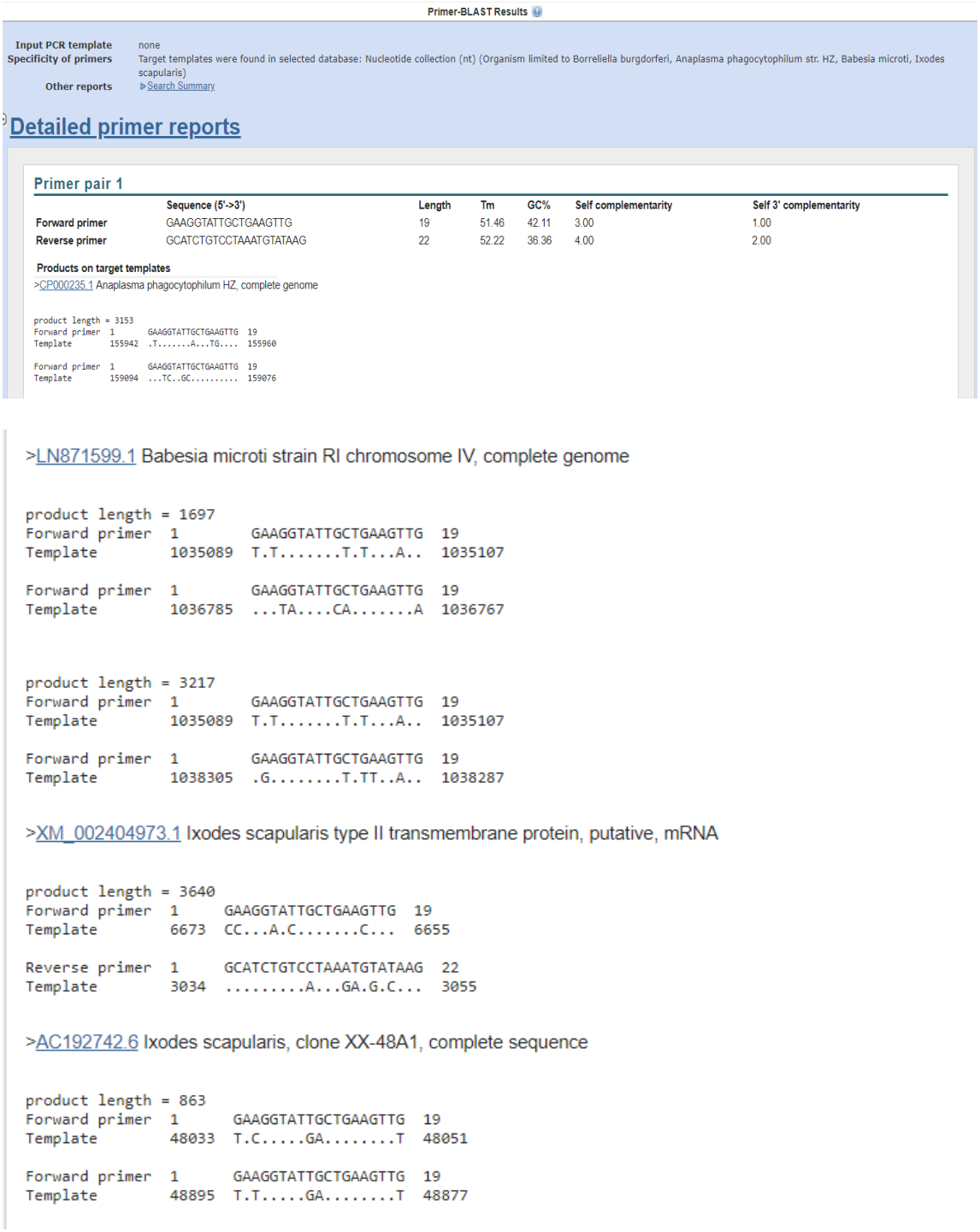

Primer-BLAST Results

Input PCR template: none
Specificity of primers: Target templates were found in selected database: Nucleotide collection (nt) (Organism limited to Borreliella burgdorferi, Anaplasma phagocytophilum str. HZ, Babesia microti, Ixodes scapularis)
Other reports: Search Summary

Detailed primer reports

Primer pair 1

	Sequence (5'->3')	Length	Tm	GC%	Self complementarity	Self 3' complementarity
Forward primer	GAAGGTATTGCTGAAGTTG	19	51.46	42.11	3.00	1.00
Reverse primer	GCATCTGTCCTAAATGTATAAG	22	52.22	36.36	4.00	2.00

Products on target templates

>CP000235.1 Anaplasma phagocytophilum HZ, complete genome

```
product length = 3153
Forward primer  1       GAAGGTATTGCTGAAGTTG  19
Template        155942  .T.......A...TG....  155960

Forward primer  1       GAAGGTATTGCTGAAGTTG  19
Template        159094  ...TC..GC..........  159076
```

>LN871599.1 Babesia microti strain RI chromosome IV, complete genome

```
product length = 1697
Forward primer  1        GAAGGTATTGCTGAAGTTG  19
Template        1035089  T.T.......T.T...A..  1035107

Forward primer  1        GAAGGTATTGCTGAAGTTG  19
Template        1036785  ...TA....CA.......A  1036767


product length = 3217
Forward primer  1        GAAGGTATTGCTGAAGTTG  19
Template        1035089  T.T.......T.T...A..  1035107

Forward primer  1        GAAGGTATTGCTGAAGTTG  19
Template        1038305  .G........T.TT..A..  1038287
```

>XM_002404973.1 Ixodes scapularis type II transmembrane protein, putative, mRNA

```
product length = 3640
Forward primer  1     GAAGGTATTGCTGAAGTTG  19
Template        6673  CC...A.C.......C...  6655

Reverse primer  1     GCATCTGTCCTAAATGTATAAG  22
Template        3034  .........A...GA.G.C...  3055
```

>AC192742.6 Ixodes scapularis, clone XX-48A1, complete sequence

```
product length = 863
Forward primer  1      GAAGGTATTGCTGAAGTTG  19
Template        48033  T.C.....GA........T  48051

Forward primer  1      GAAGGTATTGCTGAAGTTG  19
Template        48895  T.T.....GA........T  48877
```

Figure 10: Primer-BLAST results of *B. miyamotoi* primers blasted against the other tick-borne pathogens, as well as the deer tick.

The primers blast result for *B. miyamotoi* against other tick-borne pathogens recognized sequences of *A. phagocytophilum, B. microti,* and *I. scapularis* (Figure 10). It is important to note that *in silico* analysis can anticipate primer design flaws, such as binding to multiple non-intended targets. In addition, these primers performed poorly in the presence of *B. miyamotoi* DNA and were subsequently discarded from further optimization.

PART 2 - STANDARD PCR AND GEL ELECTROPHORESIS

2.1 RESULTS

Primers were tested at different concentrations (0.50-1.50 μM) and the PCR products were visualized in 2% agarose gel as described in material and methods. Each set of primers produced a single product. However, primer concentration affected the amplification efficiency for *B. microti* and *A. phagocytophilum* (Figures 11-12). The efficiency in both cases decreased at lower primer concentrations with 1.50 μM as the most optimal concentration for both *B. microti* and *A. phagocytophilum* primers. On the other hand, the efficiency of the PCR for *B. burgdorferi* and *B. miyamotoi* was not affected by primer concentration (0.5-1.50 μM) (Figures 11-12).

Considering that all PCRs amplified a single product, we decided to test these primers using a SYBR Green methodology and melt curve analysis, since our goal is to use a real-time PCR approach to detect these pathogens in ticks.

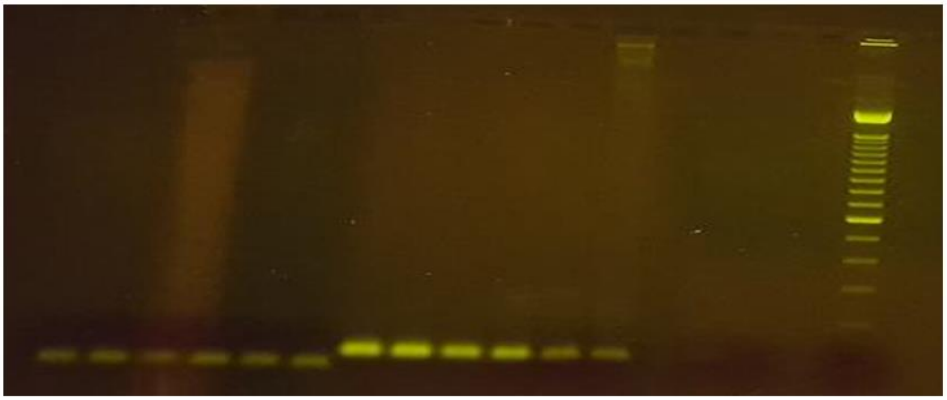

Figure 11: Gel of PCR products for *B. microti* (BM) and *B. burgdorferi* (BB).

N = Negative Control.

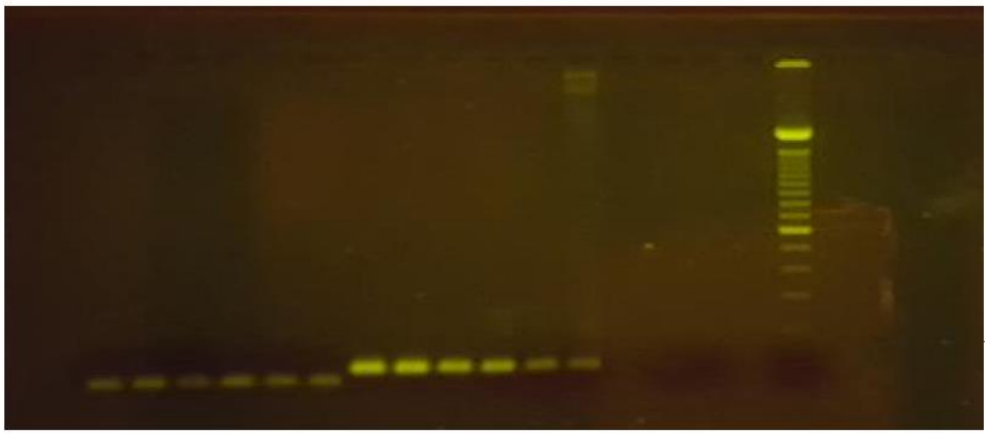

Figure 12: Gel of PCR products for *A. phagocytophilum* (AP) and *B. miyamotoi* (BM).

N = Negative Control.

PART 3 - QUANTITATIVE PCR WITH SYBR GREEN

3.1 RESULTS

The next step was to move from a conventional PCR approach to a real-time PCR since this approach is more sensitive and ultimately allows the detection of several pathogens simultaneously using a TaqMan approach. Nonetheless, before moving to a TaqMan setting, which implies the use of probes, we decided to test the efficiency of each set of primers using a SYBR Green methodology.

After testing each set of primers with their respective positive controls, we determined that one specific PCR product was formed, and that the amplification of the products was successful (Figures 13 and 15). For *B. burgdorferi*, the amplification of genomic DNA crossed the threshold at an average of 12 cycles and for *B. microti*, the amplification of plasmid DNA crossed the threshold at 25 cycles. When the PCR product was melted (Figures 14 and 16), one distinct peak is shown, indicating that the double stranded DNA of the single PCR product dissociated and became denatured.

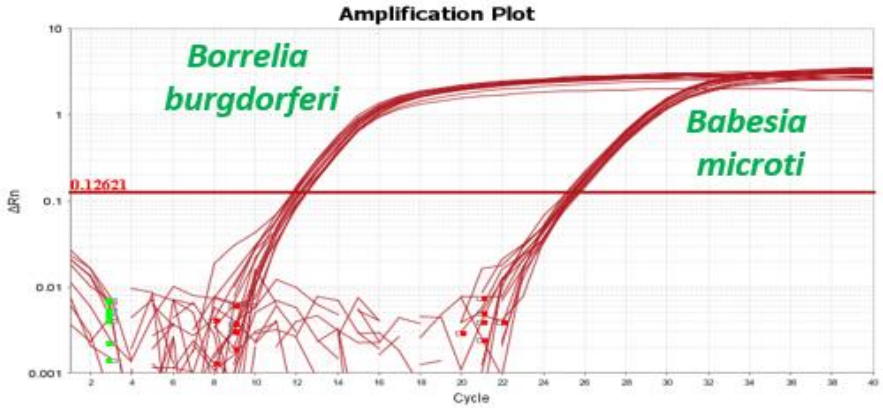

Figure 13: Amplification curves for *B. burgdorferi* and *B. microti* positive controls.

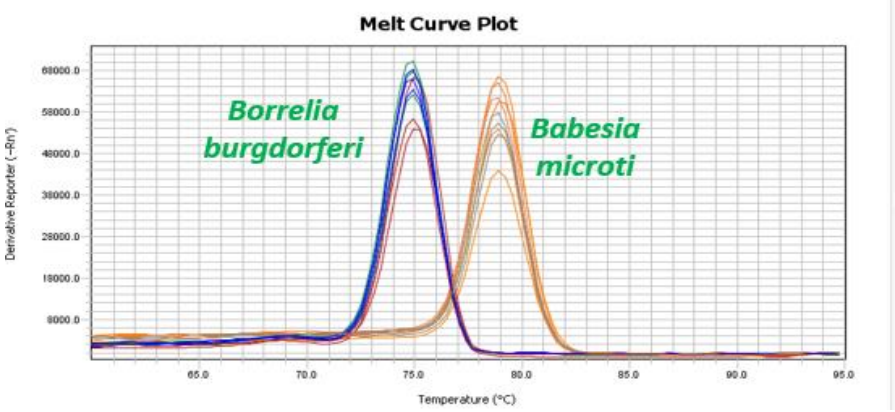

Figure 14: Melt curves for *B. burgdorferi* and *B. microti* positive controls.

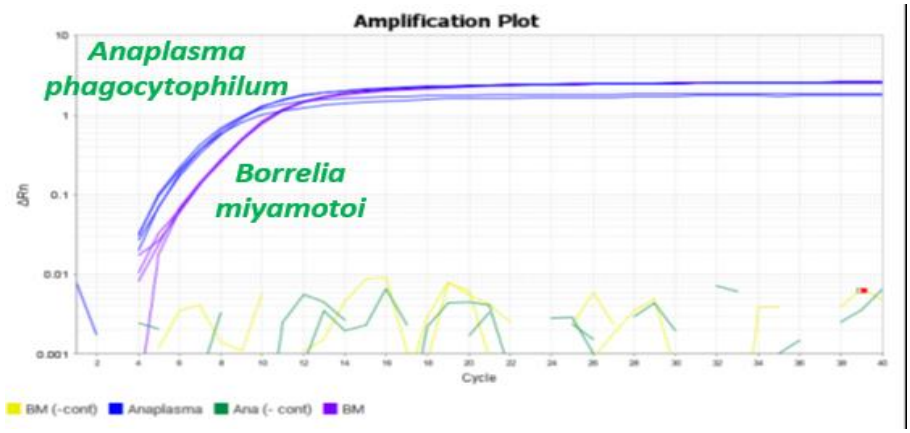

Figure 15: Amplification curves for *B. miyamotoi* and *A. phagocytophilum* positive controls.

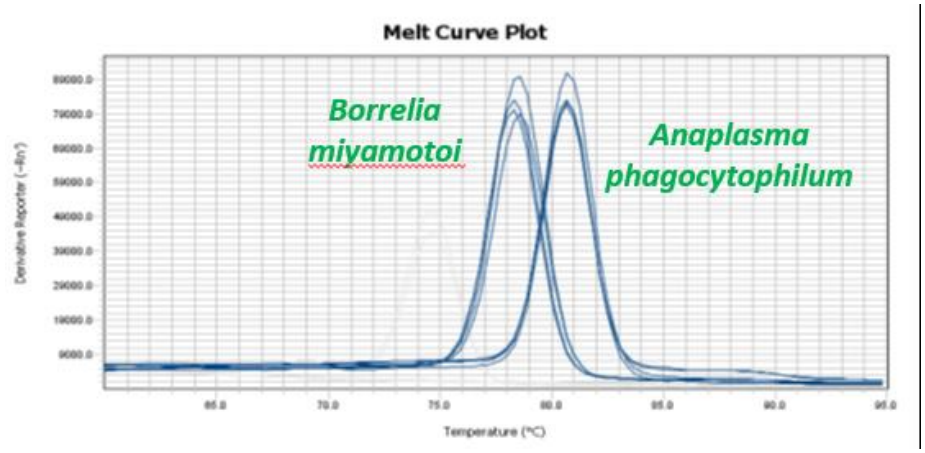

Figure 16: Melt curves for *B. miyamotoi* and *A. phagocytophilum* positive controls.

PART 4 - SYBR GREEN OPTIMIZATION

4.1 RESULTS AND OPTIMIZATION WITH FIRST PRIMER SET

4.1.1 BORRELIA BURGDORFERI

The best results were obtained at 55 °C with an efficiency of 98.125% using 1.00 μM primers, which falls within the acceptable range for amplification (Figure 17). In an ideal scenario, the efficiency of a reaction should be 100% when template DNA doubles after every cycle of the PCR. However, in a laboratory setting, the efficiency can deviate from 100% due to experimental and environmental factors. Some possible experimental errors include poor primer design, poor reaction conditions, such as a non-optimal primer annealing temperature, as well as non-optimal primer concentrations. Some causes of experimental error include pipet error when creating dilutions, power loss in the laboratory causing the PCR to stop functioning in the middle of a run, as well as varying temperature and humidity conditions due to day to day weather conditions. Due to the inevitability of the presence of some of these potential errors, a reaction is deemed as acceptable in the range of 90-110% and is considered marginally acceptable as low as 80% or as high as 120% (61).

For this tick-borne pathogen, the standard curve had a R-squared value of 0.997, which supports that dilutions were accurate (Figure 19) and only one product was formed (Figure 18). The limit of detection for this set of primers was estimated at 50 copies of the *ospA* gene. When dilutions below 50 copies were ran on the real-time PCR, no amplification occurred. No troubleshooting was needed for this tick-borne pathogen.

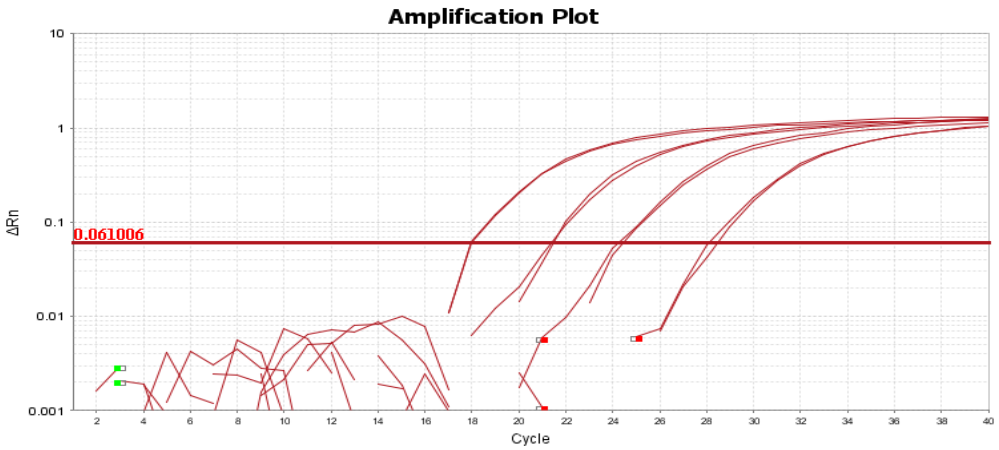

Figure 17: Amplification curve of *B. burgdorferi* serially diluted positive control genomic DNA with SYBR Green.

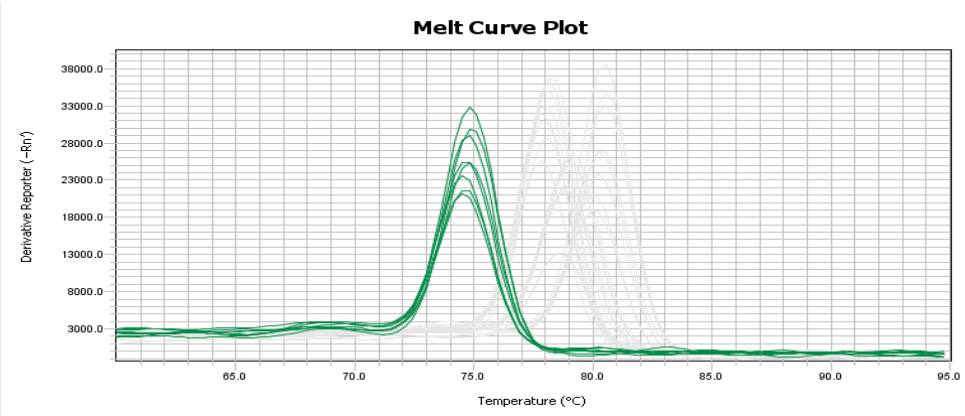

Figure 18: Melt curve of *Borrelia burgdorferi* serially diluted positive control genomic DNA with SYBR Green.

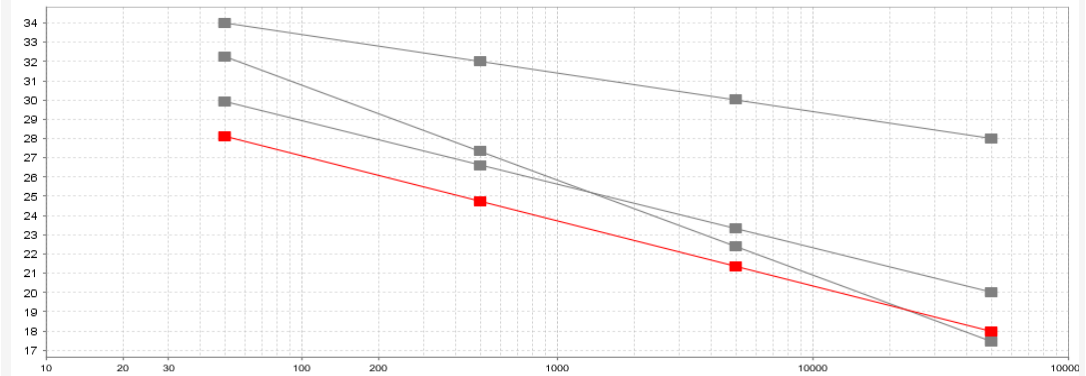

Reporter	Target	Slope	Y-Intercept	R^2	Efficiency(%)
SYBR	B bur	-3.368	33.817	0.997	98.125

Figure 19: Standard curve of *Borrelia burgdorferi* serially diluted positive control genomic DNA with SYBR Green. The y-axis denotes cycle number and the x-axis denotes copy number.

4.1.2 ANAPLASMA PHAGOCYTOPHILUM

Serially diluted positive control plasmid DNA (50,000-50 copies) with 1.00 µM primers targeting the *msp2* gene (Table 2) with an annealing temperature of 59 °C resulted in poor amplification and a reaction efficiency of 59.302%. Even though the R-squared value was 0.941, the amplification curves were disorderly, suggesting that further optimization was needed. One explanation for this low efficiency is that the primer concentrations were too high since typically pre-designed SYBR Green assays from Thermo Fisher Scientific use primer concentrations lower than 1.00 µM. Another possibility was that the annealing temperature of 59 °C was not the most optimal. Finally, it was also possible that the serial dilutions had a large amount of experimental error, which resulted in the amplification curves to not be cleanly separated.

To test these hypotheses, different tests were performed in parallel. In one experiment, a temperature gradient from 52 °C to 62 °C in 2 °C increments were chosen using two different primer concentrations - 0.500 µM and 0.250 µM. This was to determine the most optimal annealing temperature and to analyze different primer concentrations. The results are summarized in Table 15.

Table 15: *A. phagocytophilum* positive control plasmid optimization.

Annealing Temperature (°C)	**Efficiency (%) with 0.500µM Primers**	**Efficiency (%) with 0.250 µM Primers**
52	67.092	68.799
54	65.497	77.977
56	79.471	78.496
58	80.341	81.147
60	82.379	84.982
62	82.761	84.393

The best amplification results for the primers that targeted the *msp2* gene were obtained at 60 °C and 62 °C with efficiencies of 84.982% and 84.393% using primers at 0.250 µM. However, the R-squared values of the dilutions were 0.893 and 0.897 respectively, indicating that they were not accurate. Since we determined that the most optimal annealing temperature was around 60 °C - 62 °C, further primer dilutions (0.050 µM-0.250 µM) were tested at 60 °C and 62 °C to look at the effect of the efficiency with even lower primer concentrations (Table 16). To be sure the dilutions were as accurate as

possible, the dilutions were created in a separate laboratory sitting than the PCR step. The best amplification results of this experiment were obtained at 60 °C with an efficiency of 86.059% using 0.100 µM primers. Even though the R-squared value improved to 0.951 indicating that the dilutions were accurate, the efficiency was still lower than 90% - the threshold for real-time PCR.

Table 16: *A. phagocytophilum* positive control plasmid optimization continued.

Annealing Temperature (°C)	**Efficiency (%) with 0.250 µM Primers**	**Efficiency (%) with 0.125 µM Primers**	**Efficiency (%) with 0.100 µM Primers**	**Efficiency (%) with 0.050 µM Primers**
60	70.721	80.516	86.059	83.991
62	75.866	83.999	82.304	70.109

Since the reaction efficiencies were still low across all primer concentrations, the original experiment was tried again with an increased annealing temperature of 60 °C and 1.00 µM primers, the most optimal conditions from the previous experiments. Similarly, to the previous trial, the serial DNA dilutions were made in a separate laboratory sitting to minimize error throughout the experiment. The reaction efficiency of this trial increased to 91.090%, which falls within the acceptable range for amplification (Figure 20). In addition, the standard curve had a R-squared value of 0.990, which supports that dilutions were accurate (Figure 21) and only one product was formed (Figure 22). The limit of detection for this set of primers was estimated at 50 copies of the *msp2* gene.

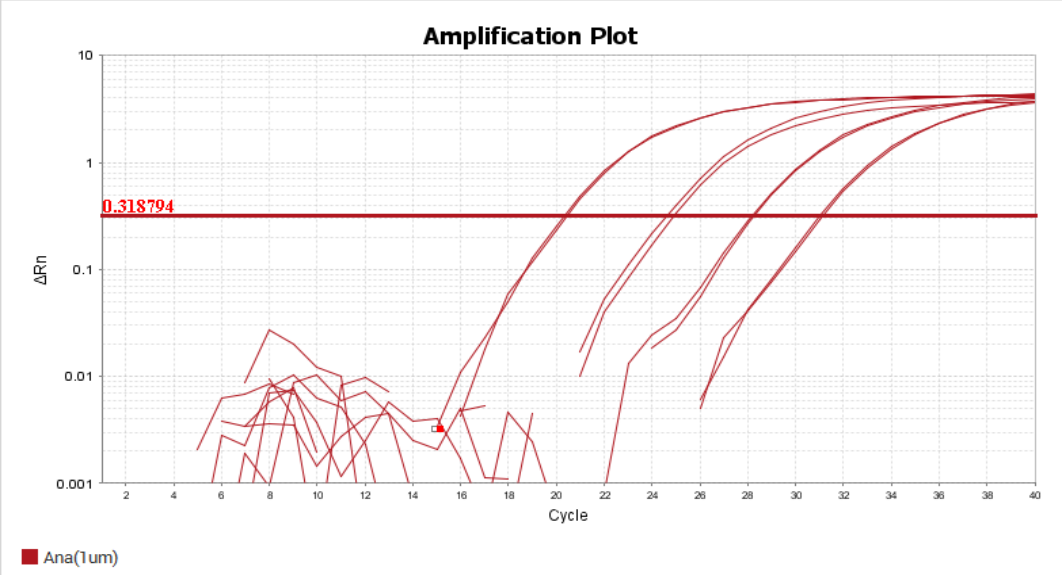

Figure 20: Amplification curve of *A. phagocytophilum* serially diluted positive control plasmid DNA with SYBR Green.

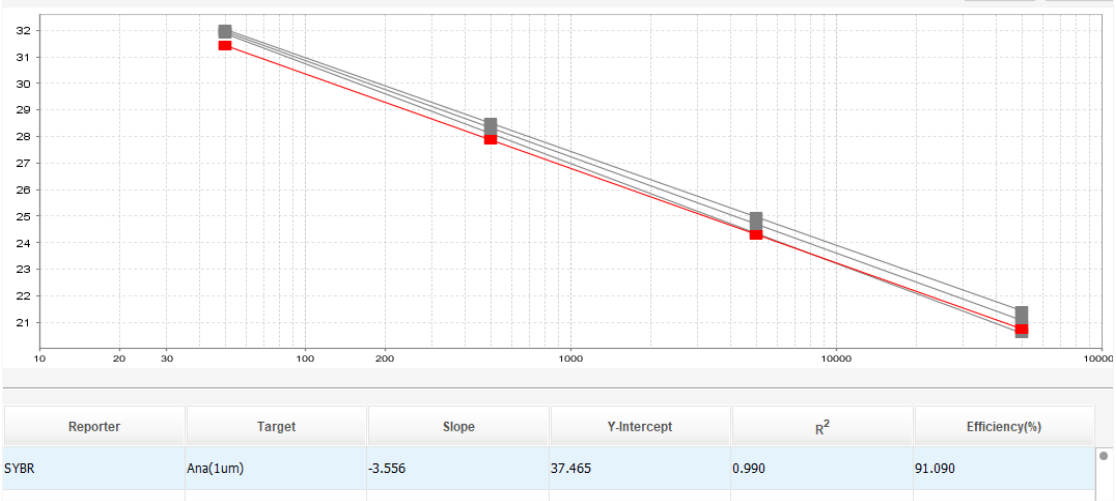

Reporter	Target	Slope	Y-Intercept	R^2	Efficiency(%)
SYBR	Ana(1um)	-3.556	37.465	0.990	91.090

Figure 21: Standard curve of *A. phagocytophilum* serially diluted positive control plasmid DNA with SYBR Green. The y-axis denotes cycle number and the x-axis denotes copy number.

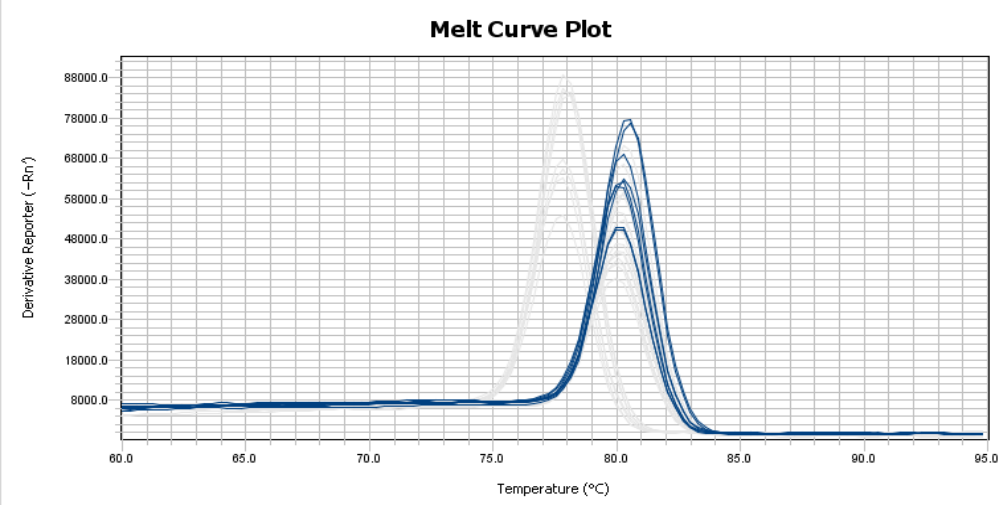

Figure 22: Melt curve of *A. phagocytophilum* serially diluted positive control plasmid DNA with SYBR Green.

4.1.3 BORRELIA MIYAMOTOI

The best amplification results for the primers that targeted the gene *glpQ* from *B. miyamotoi* (Table 2) were obtained at 57 °C with an efficiency of 91.961% using 1.00 µM primers, which falls within the acceptable range for amplification (Figure 23). In addition, the standard curve had a R-squared value of 0.999, which supports that dilutions were accurate (Figure 25) and only one product was formed (Figure 24). The limit of detection for this set of primers was estimated at 50 copies of the *glpQ* gene. No troubleshooting was needed for this tick-borne pathogen.

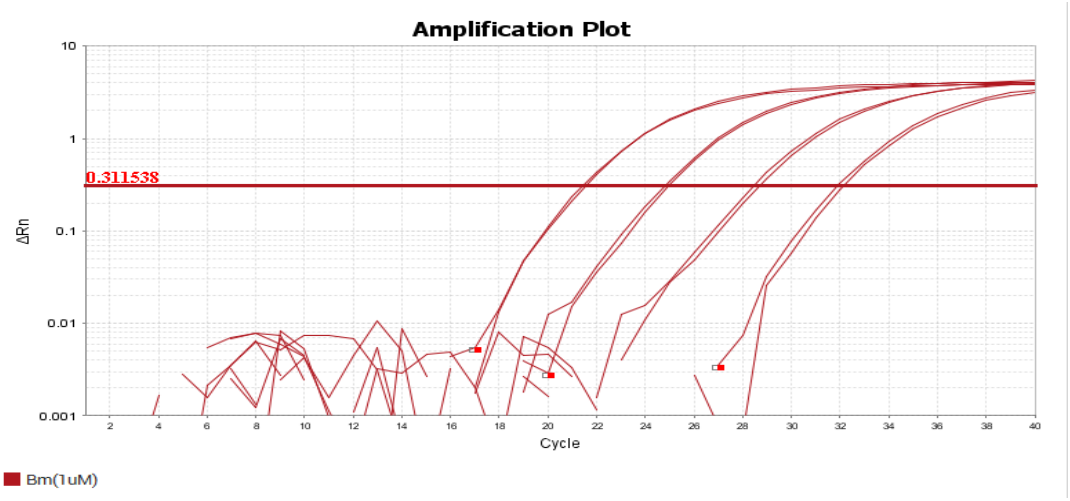

Figure 23: Amplification curve of *B. miyamotoi* serially diluted positive control plasmid DNA with SYBR Green.

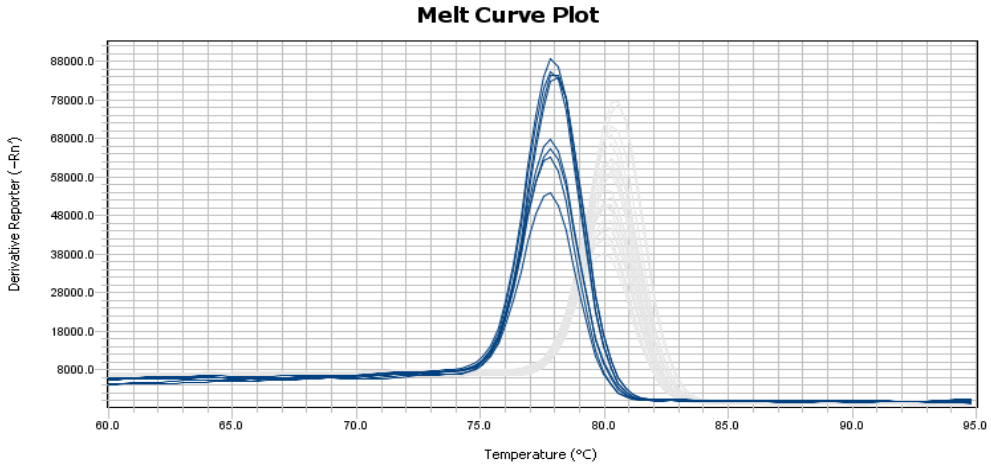

Figure 24: Melt curve of *B. miyamotoi* serially diluted positive control plasmid DNA with SYBR Green.

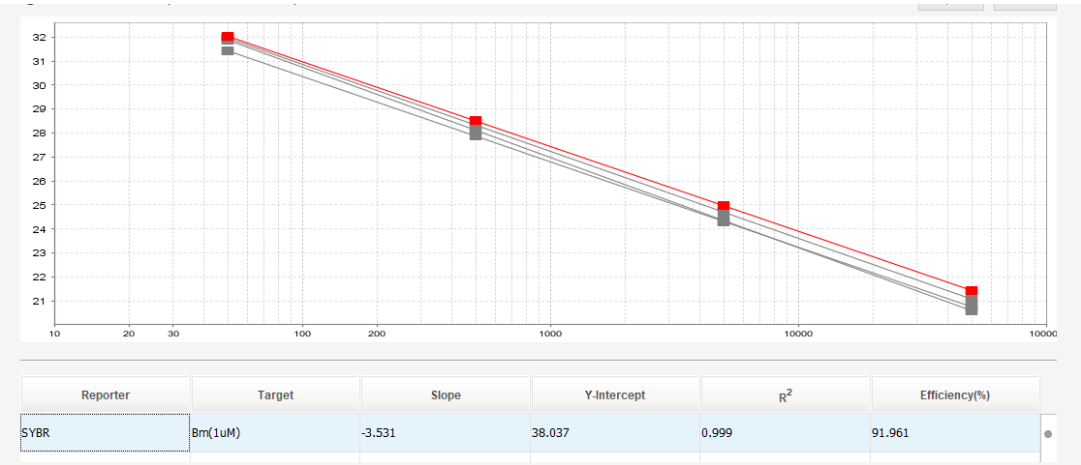

Reporter	Target	Slope	Y-Intercept	R^2	Efficiency(%)
SYBR	Bm(1uM)	-3.531	38.037	0.999	91.961

Figure 25: Standard curve of *B. miyamotoi* serially diluted positive control plasmid DNA with SYBR Green. The y-axis denotes cycle number and the x-axis denotes copy number.

4.1.4 BABESIA MICROTI

Serially diluted positive control plasmid DNA (50,000-50 copies) with 1.00 µM primers targeting the 18S rRNA gene (Table 2) with an annealing temperature of 56 °C resulted in poor amplification and a reaction efficiency of 215.719%. One explanation for this high efficiency is that there may have been an excess of DNA causing a polymerase inhibition, as well as poor primer concentrations and annealing temperature conditions. Another explanation is that there was experimental error in this trial – since the R-squared value was 0.932, the pipet error along with machine error could have caused the efficiency to be higher than it was supposed to have been.

To test these hypotheses, two different experiments were run in parallel with one another. In the first experiment, a temperature gradient from 52 °C to 60 °C in 2 °C increments was chosen using two different primer concentrations 0.500 µM and 0.250 µM. The results are summarized in Table 17. In the second experiment, the original experiment with 1.00 µM primers was repeated with newly created serial dilutions and

the annealing temperature stayed the same. During the laboratory preparations for this trial, the serially diluted DNA dilutions were created in a separate laboratory sitting to be sure that they were as accurate as possible.

Table 17: *B. microti* positive control plasmid optimization.

Annealing Temperature (°C)	**Efficiency (%) with 0.500 µM Primers**	**Efficiency (%) with 0.250 µM Primers**
52	164.999	135.691
54	152.269	126.702
56	157.751	130.348
58	170.270	148.944
60	175.709	142.521

The best amplification result of primers targeting the 18S rRNA gene in the temperature gradient experiment was obtained at 54 °C with an efficiency of 126.702% using primers at 0.250 µM. However, this is still outside the acceptable range of 90-110% and could have been due to an excess of PCR inhibitors. The efficiency also improved with a lower primer concentration, even though the amplification curves of the serial dilutions were not clean and the R-squared values decreased from the original trial. Further primer dilutions (0.050 µM-0.125 µM) were tested at 54 °C, 55 °C, and 56 °C (Table 18). Even though the efficiency of the reactions with the 0.125 µM primers at 55 °C was above 95%, pipetting error in the dilutions was evident from the unclean amplification curve, as well as the R-squared value of 0.888.

Table 18: *B. microti* positive control plasmid optimization continued.

Annealing Temperature (°C)	**Efficiency (%) with 0.125µM Primers**	**Efficiency (%) with 0.100 µM Primers**	**Efficiency (%) with 0.050 µM Primers**
54	81.743	75.871	-100.000
55	95.059	86.551	61.642
56	87.725	54.386	N/A

After re-doing the dilutions by creating them separately before the PCR step and retesting the primers at 1.00 µM at 55 °C in the second experiment, the efficiency increased to 90.143%, which falls within the acceptable range for amplification (Figure 26). In addition, the standard curve had an R-squared value of 0.990, which supports that the dilutions were more accurate than the lower-concentration primer trials (Figure 28) and only one product was formed (Figure 27). Therefore, we determined that the 1.00 µM primers at 55 °C was the most optimal PCR reaction conditions for this gene. The limit of detection for this set of primers was 50 copies of the 18S rRNA gene.

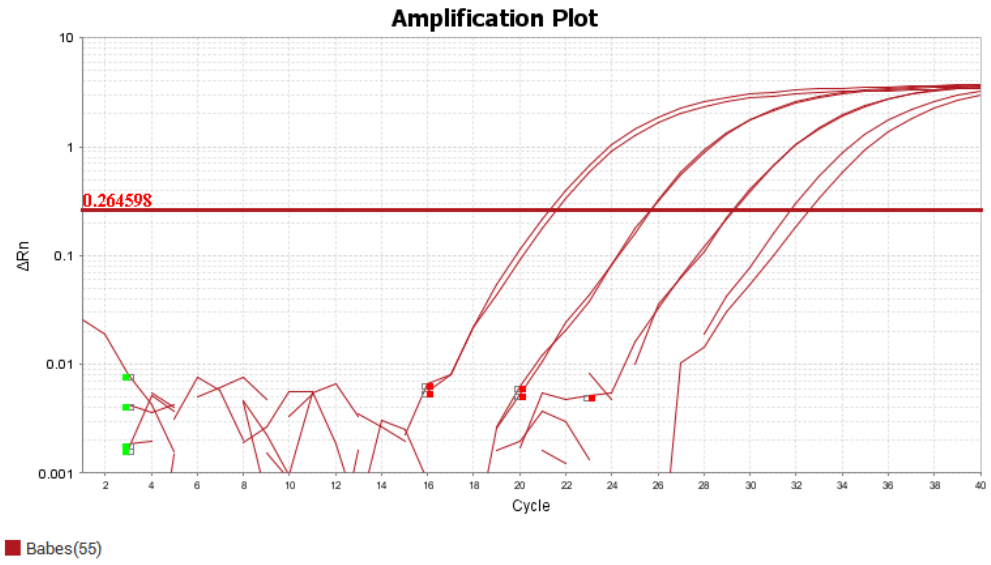

Figure 26: Amplification curve of *B. microti* serially diluted positive control plasmid DNA with SYBR Green.

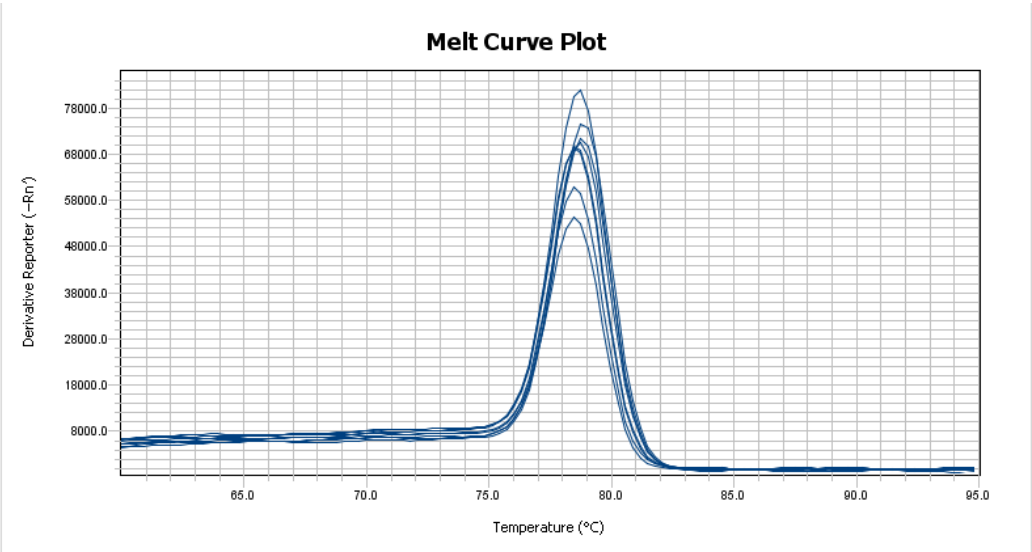

Figure 27: Melt curve of *B. microti* serially diluted positive control plasmid DNA with SYBR Green.

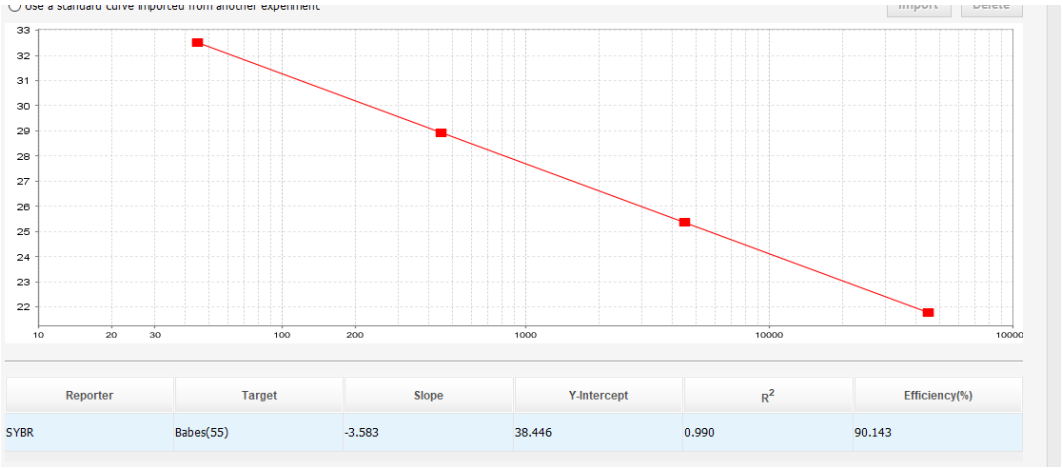

Reporter	Target	Slope	Y-Intercept	R^2	Efficiency(%)
SYBR	Babes(55)	-3.583	38.446	0.990	90.143

Figure 28: Standard curve of *B. microti* serially diluted positive control plasmid DNA with SYBR Green. The y-axis denotes cycle number and the x-axis denotes copy number.

4.2 RESULTS AND OPTIMIZATION WITH SECOND PRIMER SET

4.2.1 ANAPLASMA PHAGOCYTOPHILUM

Serially diluted positive control plasmid DNA (50,000-50 copies) combined with 1.00 µM primers targeting the *msp2* gene (Table 3), had poor reaction efficiency at annealing temperatures of 54, 55, and 56 °C (Table 19). The best results were obtained at 55 °C with an efficiency of 64.875% using primers at 1.00 µM, but the amplification curves were not cleanly separated from one dilution to the next. First, we hypothesized that the annealing temperatures were incorrect and after re-analyzing the Certificate of Analysis for the primers supplied by Thermo Fisher Scientific, we determined that the annealing temperature was too high since the melting temperature of the primers was about 50 °C. We also hypothesized that the primer concentrations were too high. To test these hypotheses, the first trial had less concentrated primers at 0.50 µM, 0.250 µM, and 0.125 µM tested at 45 °C. The results of this trial indicated no amplification except with the 50,000 and 5,000 copy number dilutions.

For the second trial, a temperature gradient from 39 °C to 51 °C in 2 °C increments (omitting the already tested 45 °C) using 0.250 μM since we still hypothesized that the primer concentration was too high. Additionally, the positive control plasmid DNA dilutions were extended to include 500,000 copies, as we hypothesized that the dilution range could have been too small. The results of this trial were worse than the previous with no amplification at 43-51 °C, only 500,000-50,000 copies of plasmid DNA amplified at 41 °C, and only 500,000 opies of plasmid DNA amplified at 39 °C. As a final optimization attempt, the primer concentration was increased (1.00 and 0.50 μM) and tested at higher annealing temperatures (52, 53, and 54 °C), but the DNA dilutions were created in a separate laboratory sitting to be sure they were as accurate as possible. After running the PCR at a different laboratory sitting, this optimization gave an efficiency of 90.892% with a primer concentration of 1.00 μM with an annealing temperature of 53 °C.

Table 19: *A. phagocytophilum* positive control plasmid optimization continued.

Annealing Temperature (°C)	**Efficiency (%) with 1.00 μM Primers**
54	51.452
55	64.875
56	61.736

4.2.2 BABESIA MICROTI

Serially diluted positive control plasmid DNA (50,000-50 copies) combined with 1.00 μM primers targeting the 18S rRNA gene (Table 3), had poor reaction efficiency at annealing temperatures of 54, 55, and 56 °C (Table 20). The best results were obtained at 54 °C with an efficiency of 59.330% using primers at 1.00 μM. We hypothesized that the annealing temperatures were incorrect and after re-analyzing the Certificate of Analysis for the primers supplied by Thermo Fisher Scientific, we determined that the annealing temperature was too high since the melting temperature of the primers was about 50 °C. We also hypothesized that the primer concentrations were too high. To test these hypotheses, the first trial had less concentrated primers at 0.50 μM, 0.250 μM, and 0.125 μM tested at 45 °C, along with a re-do of the 1.00 μM primers.

The results of this trial (Table 21) showed no amplification of the 500 and 50 copy plasmid dilutions and the efficiency was poor for the copy number dilutions that did amplify. The best results were obtained with the 1.00 μM primers with an efficiency of 49.433%, even though only the highest copy number dilutions amplified. We hypothesized that the 1.00 μM primers were the most optimal, but that the annealing temperature could be improved. To test this hypothesis, a temperature gradient from 47°C to 53 °C in 2 °C increments were chosen for the next optimization trial using a primer concentration of 1.00 μM. The results showed that none of the copy number plasmid dilutions were detectable by the machine, and these primers were discarded.

Table 20: *B. microti* positive control plasmid optimization continued.

Annealing Temperature (°C)	**Efficiency (%) with 1.00 µM Primers**
54	59.330
55	49.047
56	51.333

Table 21: *B. microti* positive control plasmid optimization continued with 45 °C annealing temperature.

Primer Concentration (µM)	**Efficiency (%)**
1.00	49.433
0.50	46.575
0.25	44.094
0.125	-100.000

.

4.2.3 BORRELIA BURGDORFERI

Serially diluted positive control genomic DNA (50,000-50 copies) combined with 1.00 µM primers targeting the *ospA* gene (Table 3), resulted in no amplification of DNA. We hypothesized that the positive control was not diluted correctly, as it was a new vial, or that the primers were not binding to the template DNA. To test these hypotheses, the new primers (1.00 µM) were tested with the old genomic DNA control serially diluted (50,000-50 copies) and only slight amplification was seen in the 500,000 and 50,000

copy dilutions – not even crossing the threshold. We also hypothesized that the 45 ℃ annealing temperature was not the most optimal. To test this hypothesis, the 1.00 μM primers were tested at different annealing temperatures (57, 59, and 61 ℃) and no amplification of the DNA occurred. Therefore, these primers were deemed no good.

4.2.4 BORRELIA MIYAMOTOI

Serially diluted positive control plasmid DNA (500,000-50 copies) combined with 1.00 μM primers targeting the *glpQ* gene (Table 3), resulted in no amplification of DNA below 500 copies. We hypothesized that the annealing temperature was not optimal. To test this hypothesis, a temperature gradient from 42℃ to 54 ℃ in 2 ℃ increments was chosen for the next optimization trial using a primer concentration of 1.00 μM. The 54 ℃ annealing temperature resulted in amplification of all copy number dilutions with an efficiency of 58.457%. Since the efficiency was low, it was hypothesized that the primer concentration was too high. To test this, primer concentration was redused to 0.50 μM and the amplification was even poorer. As a final resort, the primer concentrations were increased back to 1.00 μM and the annealing temperatures were increased (57, 59, and 61 ℃) and no amplification occurred. The results of this trial indicated that the machine could not detect a PCR product below 50,000 copies and thus, these primers were discarded.

PART 5 – COMPARISON OF GEL ELECTROPHORESIS AND SYBR GREEN – FIRST SET OF PRIMERS WITH CLIENT TICKS

5.1 RESULTS

To compare both the gel electrophoresis and SYBR Green methodologies, four client ticks (named R, S, T, and U to protect client privacy) were tested, and the results can be seen in table 22. For these pathogens, only *B. burgdorferi, B. microti*, and *A. phagocytophilum* were tested since the lab was not providing clients with screening against *B. miyamotoi* at the time. As it can be seen from table 22, all four of the client deer ticks were negative for all tick-borne pathogens except for client tick (R) that was positive for *B. microti* in both the gel electrophoresis and SYBR Green methodologies.

Table 22: Client deer ticks tested in both the gel electrophoresis and SYBR Green methodologies along with their presence or absence of the tick-borne pathogens.

Tick-Borne Pathogen		***B. burgdorferi***		***B. microti***		***A. phagocytophilum***	
PCR Method		Standard	Real Time	Standard	Real Time	Standard	Real Time
Client Tick	R			X	X		
	S						
	T						
	U						

X = Positive for that tick-borne pathogen

Since both methodologies provided the same results, the gel electrophoresis methodology was stopped to resume a full-time commitment with the SYBR Green methodology, as well as further research on migrating to a TaqMan multiplex methodology in the future.

5.2 TROUBLESHOOTING

During verification of the ticks on both the gel electrophoresis and SYBR Green methodologies, it was difficult to verify the presence or absence of the PCR products on the gel with the naked eye due to their small amplicon lengths. That is one of the benefits of the real-time PCR and its ability to detect PCR products with small amplicon lengths. Therefore, not many ticks were able to be tested on both methodologies due to a large percentage of human error in being able to identify the presence of very faint bands on the gel. Additionally, potential contamination was detected in tick samples that turned to be positive for all pathogens. The negative control with no tick DNA added was negative, suggesting that the contamination was during the extraction process and not the PCR component. To avoid using contaminated buffers, a new DNA extraction kit was purchased. In addition, new primer dilutions were done from stocks and new SYBR Green master mix was purchased. Once the old reagents were swapped for new ones, the contamination problem was resolved.

PART 6 – SYBR GREEN – FIRST SET OF PRIMERS WITH CLIENT TICKS

6.1 RESULTS

Over the span of the duration of this project, 158 client deer ticks were verified for the presence of their tick-borne pathogens with the SYBR Green methodology. Their results are documented in table 24 below along with the total percentage of ticks diseased (Table 23).

Table 23: Total number of client deer ticks with a tick-borne disease, along with the total number of ticks tested and the percentage of deer ticks diseased determined with the SYBR Green methodology.

Pathogen	***B. burgdorferi***	***B. microti***	***B. miyamotoi***	***A. phagocytophilum***
Total with TBD	18	10	11	17
Total Ticks Tested	158	158	158	158
Percentage Diseased (%)	11.39	6.33	6.96	10.76

Table 24: Individual client ticks along with their presence or absence of the tick-borne pathogens.

Client Tick	***B. burgdorferi***	***B. microti***	***B. miyamotoi***	***A. phagocytophilum***
A		X		X
B				
C				
D				
E		X		
F	X			
G				
H				
I				
J	X			
K	X			
L				
M				
N				
O				
P				X
Q				
R				X
S				X

T				
U				
V	X			
W				X
X	X			X
Y	X	X		
Z				
A1	X		X	X
B1	X		X	X
C1			X	X
D1				
E1			X	
F1			X	X
G1				X
H1				
I1			X	
J1	X		X	X
K1		X		
L1				
M1				
N1				
O1				
P1				

Q1				X
R1				
S1				
T1	X			X
U1				
V1	X		X	
W1	X			
X1		X		
Y1				
Z1				
A2				
B2				
C2				
D2				
E2				
F2		X		
G2				
H2				
I2				
J2				
K2				
L2				
M2				

N2				
O2		X		
P2				
Q2				
R2	X			
S2	X			
T2				
U2				X
V2				
W2				
X2				
Y2				
Z2				
A3				
B3				
C3				
D3				
E3				
F3				
G3				
H3				
I3				
J3				

K3				
L3				
M3	X			
N3				
O3				
P3				
Q3	X			
R3				
S3				
T3				
U3				
V3				
W3				
X3				
Y3				
Z3				
A4				
B4				
C4				
D4	X			
E4				
F4				
G4				

H4				
I4		X	X	
J4			X	
K4				
L4				
M4				
N4				
O4		X		
P4				
Q4				
R4				
S4				
T4				
U4				
V4				
W4				
X4				
Y4				
Z4				
A5				
B5				X
C5				
D5				

E5				
F5				
G5				
H5				
I5				
J5			X	
K5				
L5				
M5		X		
N5				
O5	X			
P5				
Q5				
R5				
S5				
T5				X
U5				
V5				
W5				
X5				
Y5				
Z5				
A6				

B6				
C6		X		X
D6				
E6				
F6				
G6		X		
H6	X			
I6				
J6				
K6				
L6	X			
M6	X			
N6				
O6				
P6				
Q6				
R6				X
S6				
T6				X
U6				X
V6				
W6				
X6	X			

Y6				X
Z6	X			X
A7	X	X		
B7				

X = Positive for that tick-borne pathogen

Based on the 158 client deer ticks tested for their tick-borne pathogens (Table 23), 18 out of 158 tested positive for the presence of *B. burgdorferi* (11.39%), 10 out of 158 tested positive for the presence of *B. microti* (6.33%), 11 out 158 tested positive for the presence *B. miyamotoi* (6.96%), and 17 out of 158 tested positive for the presence of *A. phagocytophilum* (10.76%).

6.2 OVERALL DETECTION OF TICKS

When comparing these experimental results with other tick-borne pathogen studies conducted in the New Jersey/New York area, some comparisons can be made. In this study, about 11% of the deer ticks tested positive for *A. phagocytophilum*. This is similar to a study conducted on *I. scapularis* adult ticks from the New York area that also resulted in 11% positive for this tick-borne disease (67). However, in studies conducted with deer ticks from New Jersey, there seems to be a variation of percentages ranging from about 2% to 6% of deer ticks positive for this tick-borne disease (68-71). One reason why the percentage of ticks with *A. phagocytophilum* was more similar to the New York percentage is that some clients that sent in ticks for testing were from New York and northern New Jersey where *A. phagocytophilum* seems to be more prevalent than the

southern New Jersey area. Therefore, the 11% positive for *A. phagocytophilum* is not too far out of spec.

In our experiment, about 6% of deer ticks screened positive for *B. microti*, which agrees with previous PCR studies conducted in the New Jersey area. Most studies had *I. scapularis* ticks positive with *B. microti* ranging from about 5-8% of their total sample size (67-70). Since our total percentage of deer ticks positive for *B. microti* falls in the middle of the range suggested from previous studies, this indicates that this PCR methodology is robust in providing a sound result of the presence or absence of this tick-borne pathogen.

With the two *Borrelia*s, the results of our study deviate a bit more than the studies conducted previously. First, about 7% of deer ticks in this study were positive for *B. miyamotoi*. In previous studies, the percentage positive for this tick-borne pathogen seemed to be a bit lower, ranging from about 2-3% of ticks tested (39, 42, 67, 71). However, *B. miyamotoi*, which is known to have a lower incidence than *B. burgdorferi*, was documented in about half as many deer ticks as the number of deer ticks infected with *B. burgdorferi* in our study, agreeing with that trend (42). Secondly, about 11% of deer ticks in this study were positive for *B. burgdorferi*. In previous studies, the percentage positive for this tick-borne pathogen was higher, ranging from about 20-70% of all ticks tested (67-71). Even though the percentage of deer ticks positive for Lyme disease was lower in this study compared to others, it was the most prevalent tick-borne pathogen found in the deer ticks tested for both this study, as well as all the others. This is not surprising since the CDC notes that over 30,000 cases of Lyme disease are reported each year and that this is the most prevalent tick-borne disease (38).

PART 7 – TAQMAN PROBES TESTING

7.1 RESULTS AND TROUBLESHOOTING OF THE FIRST SET OF PROBES

The first step was to choose a master mix that will give robust results. Different TaqMan master mixes from Thermo Fisher Scientific have different testing applications. For example, the TaqPath™ ProAmp™ Master Mix is used for genotyping and copy number assays, whereas the TaqMan™ Gene Expression Master Mix focuses on the amplification of genes of interest. When the TaqMan experiments began in this study, we thought that the TaqPath™ ProAmp™ Master Mix would work well because it is commonly used for copy applications. However, this master mix did not render a good result. The amplification curves were all disconnected and disorderly.

After analyzing the PCR thermocycler settings for TaqMan, it had a passive reference set to ROX that should have been set for Mustang Purple. The passive reference dye is used in PCR reactions to reduce the effect of pipetting error and other machine abnormalities. If the wrong passive reference is set, the TaqMan fluorescent dye on the probe has no form of normalization and can result in poor amplification. After changing the passive reference to Mustang Purple, the amplification results improved, but not much. Therefore, we decided to switch the master mix to one that had been validated for gene expression experiments. Additionally, we determined that the probe concentrations should have been in the 300 to 200 nM concentration range based on Thermo Fisher Scientific and their pre-designed assays. Any probe concentration lower than 200 nM could result in less efficient amplification.

The master mix was changed to TaqMan™ Gene Expression with a passive reference of ROX, 300 nM and 200 nM probes were used with standard PCR run

conditions. As seen in the following amplification plot (Figure 29), the amplification of the *B. burgdorferi* positive control was low and did not improve. The amplification normalized reporter value, or delta Rn, is small. This indicates that the fluorescent signal of the TaqMan probe normalized to the passive reference, ROX, results in a small magnitude in the amplification reaction. Even though the efficiency of this standardization was around 90%, the magnitude of the amplification curves suggests otherwise.

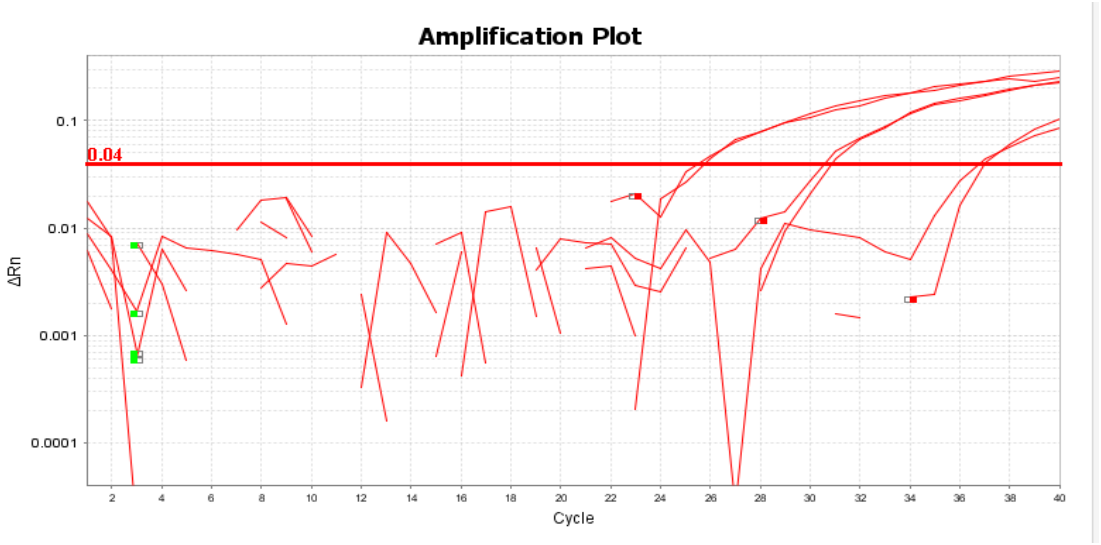

Figure 29: TaqMan amplification plot of *B. burgdorferi* positive control genomic DNA dilutions with TaqMan™ Gene Expression master mix with a probe concentration of 200 nM and primer concentrations of 1.00 µM.

For the next optimization trial, the PCR run method was changed from standard to fast. We thought that the magnitude of the amplification curves would improve to give the Taq polymerase a longer period of time to activate and improve the DNA elongation step. However, there were mixed results. The *B. burgdorferi* positive control genomic

DNA copy number dilutions did not amplify. The *B. miyamotoi* positive control plasmid DNA at 50,000 and 5,000 copies, however, did and had a reaction efficiency of around 60%. The lower number of copies (500 and 50) did not amplify (Figure 30).

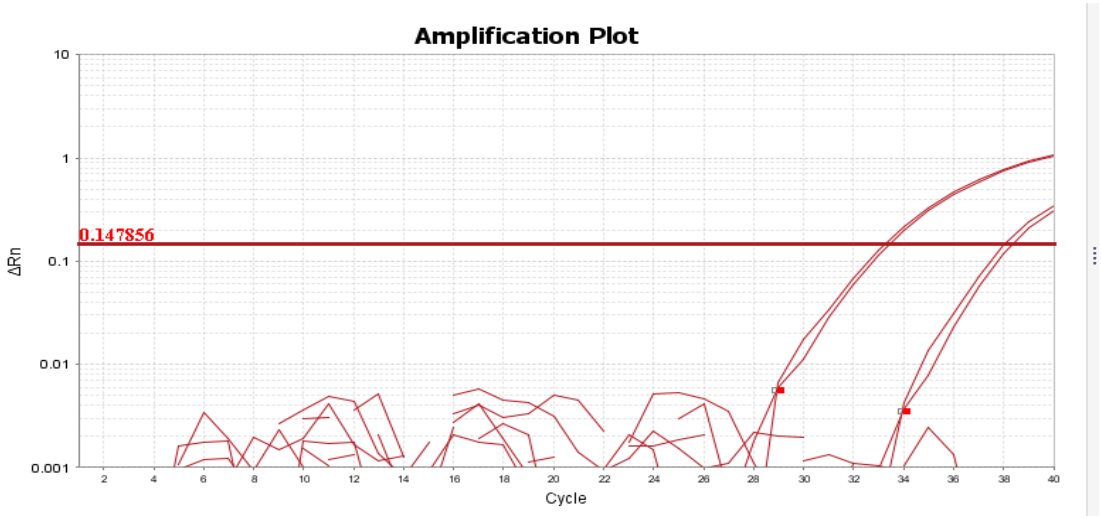

Figure 30: TaqMan amplification plot of *B. miyamotoi* positive control plasmid dilutions with TaqMan™ Gene Expression master mix with a probe concentration of 200 nM and a primer concentration of 1.00 µM.

To improve DNA amplification at lower copy number dilutions, the dilution range was increased in the next optimization trial (500,000-50 copies) of the *Borrelias*, suggesting that the machine would be able to detect lower concentrations of DNA with a wider dilution range. However, this was not the case. Based on the amplification plot for *B. burgdorferi* positive control genomic DNA (Figure 31), 500,000-5,000 copies of the positive control genomic DNA amplified. The standard curve had an efficiency of 77.223%. However, the inability to detect a copy number below 5,000 copies is a problem since the number of tick-borne pathogens present in a deer tick can be lower than 5,000 copies.

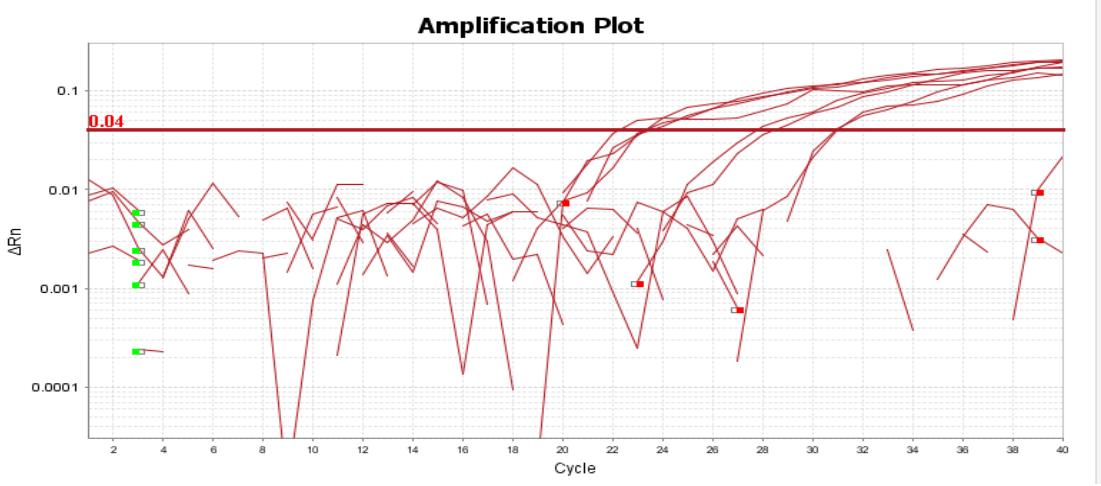

Figure 31: TaqMan amplification plot of *B. burgdorferi* positive control genomic DNA dilutions with a larger copy number range with TaqMan™ Gene Expression master mix with a probe concentration of 200 nM and primer concentrations of 1.00 µM.

To rule out machine error, a pre-optimized 18S rRNA eukaryote assay provided from Thermo Fisher Scientific was tested on deer ticks (Figure 32) and *B. microti* genomic DNA (Figure 33). Since the pre-optimized probes amplified, the machine was not to blame.

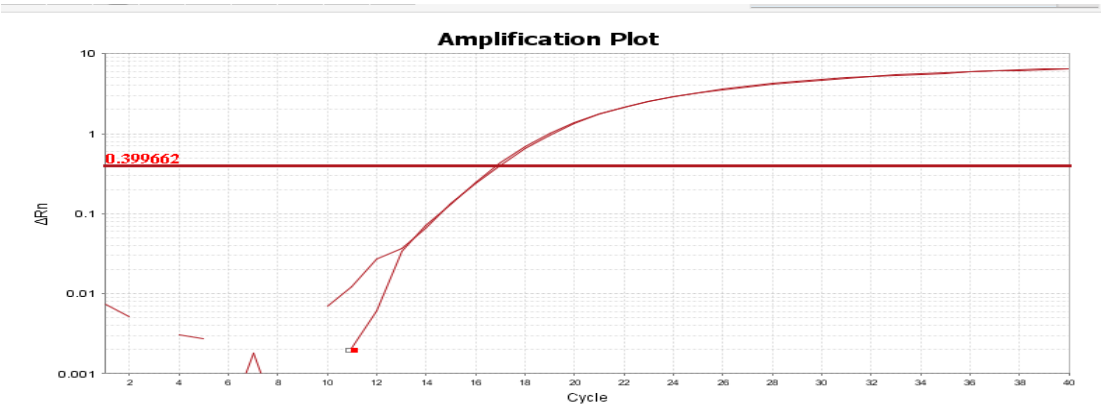

Figure 32: Deer tick extracted DNA amplified with the Thermo Fisher pre-designed TaqMan 18S rRNA Eukaryote assay.

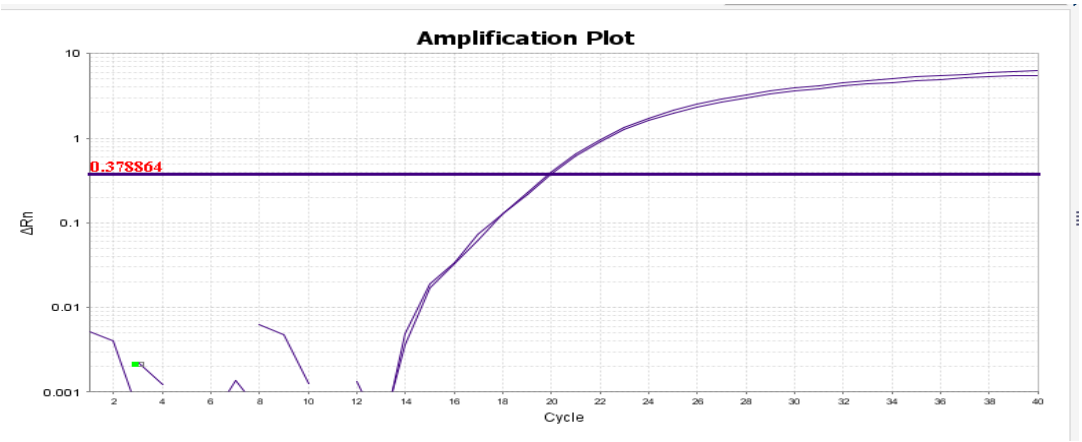

Figure 33: *B. microti* DNA amplified with the Thermo Fisher pre-designed TaqMan 18S rRNA Eukaryote assay.

As a last attempt to get the probes working, we thought that the probes were not binding to the genomic/plasmid DNA and that the DNA could have been the problem. Therefore, a different strain of *B. burgdorferi* was tried. However, no amplification occurred, and the probes were deemed not functional. New primers and probes were designed to start again.

7.2 SECOND SET OF PROBES

7.2.1 TROUBLESHOOTING

Since the original probes for the tick-borne pathogens were not working, we proceed to analyze other factors that may interfere with the performance of the PCR and perform a root-cause analysis. First, no G bases were present at the 5' end of the probe; therefore, this did not affect the quencher and the probe's ability to bind to its template

sequence. Next, the delta free energy of the probes was larger than the -9 kcal/mole limit where primer dimer interactions could have been influencing binding. It was possible that the probes were becoming degraded with the use of water that was not nuclease free, but this was not the case since the 18S pre-designed eukaryotic assay diluted with the same water worked perfectly.

Lastly, the probe melting temperatures were compared to the primer melting temperatures. For the *B. burgdorferi* FAM-QSY probe, the melting temperature was 44 °C, which was over 10 °C below the optimized primer annealing temperatures. For the *B. miyamotoi* VIC-QSY probe, the melting temperature of the probe was 53 °C which was about 5 °C below the optimized primer annealing temperatures. For the probe to bind to the template DNA, it needs a melting temperature higher than the primers, so it can bind to the DNA before the primers and DNA polymerase begin to extend the DNA. If the probe cannot bind to the template DNA, the reporter with the fluorescent dye cannot be cleaved and separate from the quencher, and no fluorescence will take place.

To solve this problem, we switched the quencher from QSY to MGB, or minor groove binder, for the two *Borrelia* probes due to the MGB quencher having the ability to increase the melting temperature of the probes by clamping the DNA and probe in place and near of one another. The original probes were picked with the QSY quencher because it was non-fluorescent and was recommended by Thermo Fisher Scientific for multiplexing. The MGB probes on the other hand are not optimized for multiplexing and have a non-fluorescent quencher similarly to the QSY probes with the MGB attached to that quencher.

7.2.2 OPTIMIZATION

7.2.2.1 BORRELIA BURGDORFERI

The best amplification results of the primers and probe targeting the *ospA* gene (Tables 2 and 4), were obtained at 55 °C with 1.00 µM primers and 250 nM probe (Figure 34) with an efficiency of 86.350% with the omission of one 500 copy technical replicate and an efficiency of 85.370% with the technical replicate included. In addition, the standard curve omitting the technical replicate had a R-squared value of 0.992 whereas the standard curve including it had a R-squared value of 0.990, which both support that the dilutions were accurate (Figures 35-36). The limit of detection for this set of primers was estimated at 50 copies of the *ospA* gene. No troubleshooting was needed for this tick-borne pathogen.

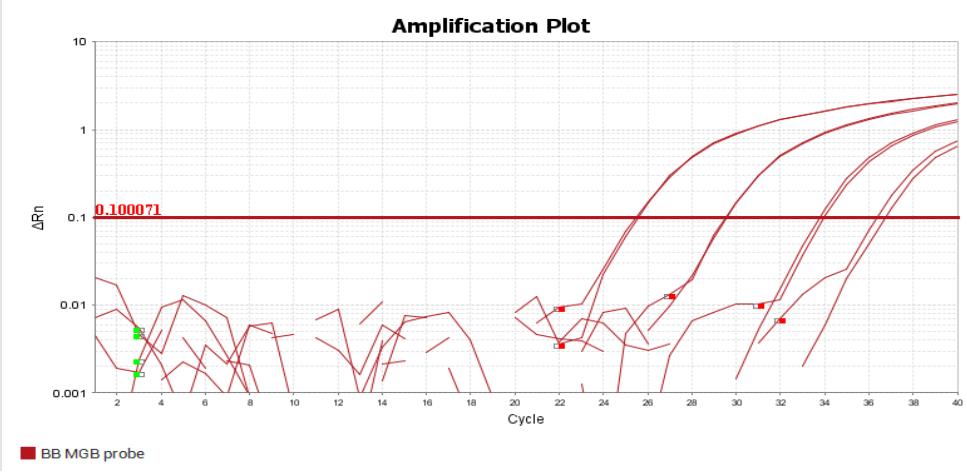

Figure 34: Amplification curve of *B. burgdorferi* serially diluted positive control genomic DNA with TaqMan MGB probe.

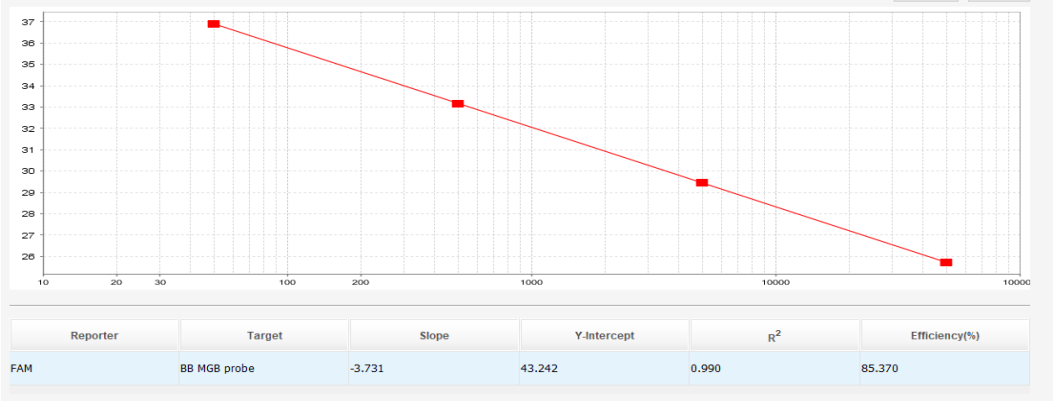

Reporter	Target	Slope	Y-Intercept	R^2	Efficiency(%)
FAM	BB MGB probe	-3.731	43.242	0.990	85.370

Figure 35: Standard curve of *B. burgdorferi* serially diluted positive control genomic DNA with TaqMan probe. The y-axis denotes cycle number and the x-axis denotes copy number. One 500 copy dilution replicate has been omitted from this analysis.

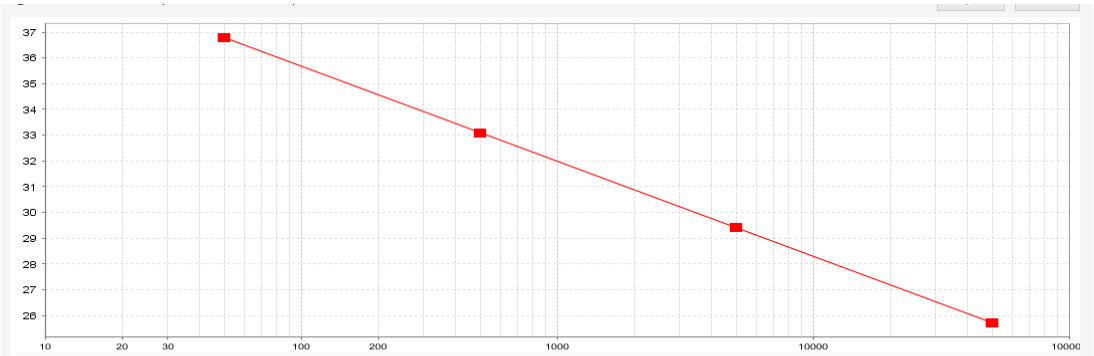

Reporter	Target	Slope	Y-Intercept	R^2	Efficiency(%)
FAM	BB MGB probe	-3.699	43.083	0.992	86.350

Figure 36: Standard curve of *B. burgdorferi* serially diluted positive control genomic DNA with TaqMan probe. The y-axis denotes cycle number and the x-axis denotes copy number. All serial dilution replicates are included.

7.2.2.2 BORRELIA MIYAMOTOI

The best amplification results of the primers and probe targeting the *glpQ* gene (Tables 2 and 4), were obtained at 57 °C with 1.00 µM primers and 250 nM probe (Figure 37) with an efficiency of 89.058% with the omission of one 50 copy technical replicate and an efficiency of 87.612% with the technical replicate included. In addition, the standard curve omitting the technical replicate had a R-squared value of 0.993 whereas the standard curve including it had a R-squared value of 0.995, which both support that the dilutions were accurate (Figures 38-39). The limit of detection for this set of primers was estimated at 50 copies of the *glpQ* gene. No troubleshooting was needed for this tick-borne pathogen.

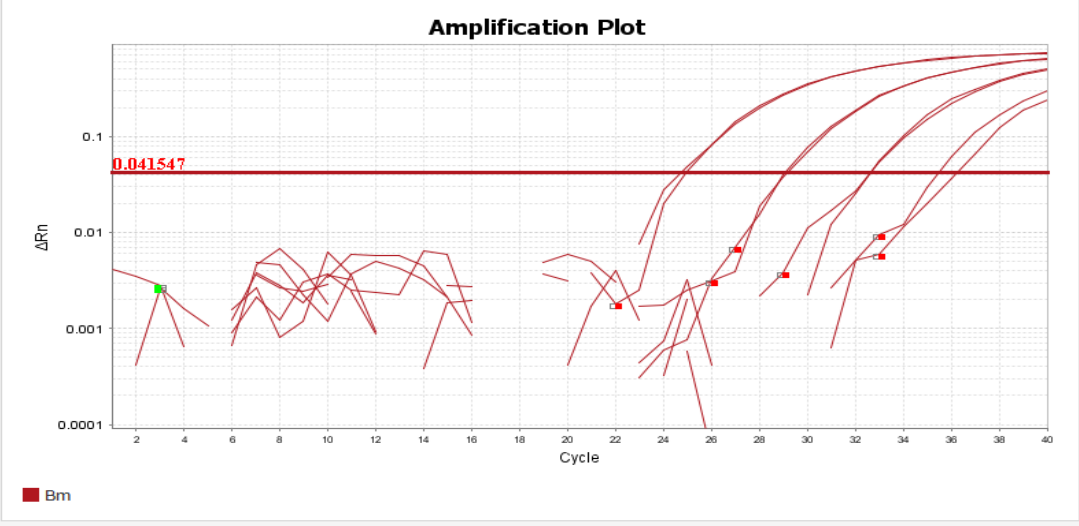

Figure 37: Amplification curve of *B. miyamotoi* serially diluted positive control plasmid DNA with TaqMan MGB probe.

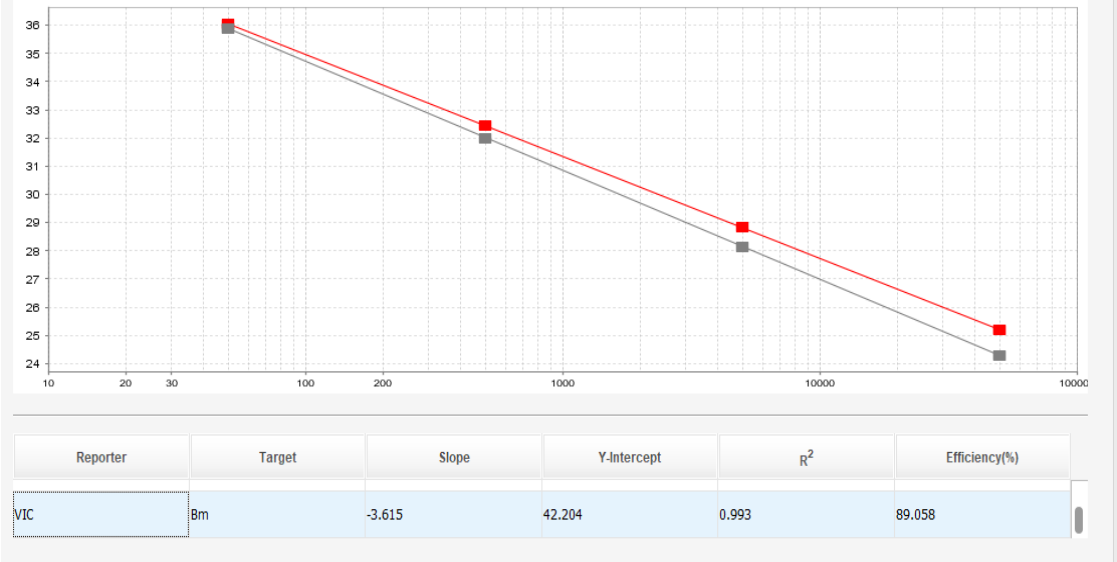

Reporter	Target	Slope	Y-Intercept	R^2	Efficiency(%)
VIC	Bm	-3.615	42.204	0.993	89.058

Figure 38: Standard curve of *B. miyamotoi* serially diluted positive control plasmid DNA with TaqMan probe. The y-axis denotes cycle number and the x-axis denotes copy number. One 50 copy dilution replicate has been omitted from this analysis.

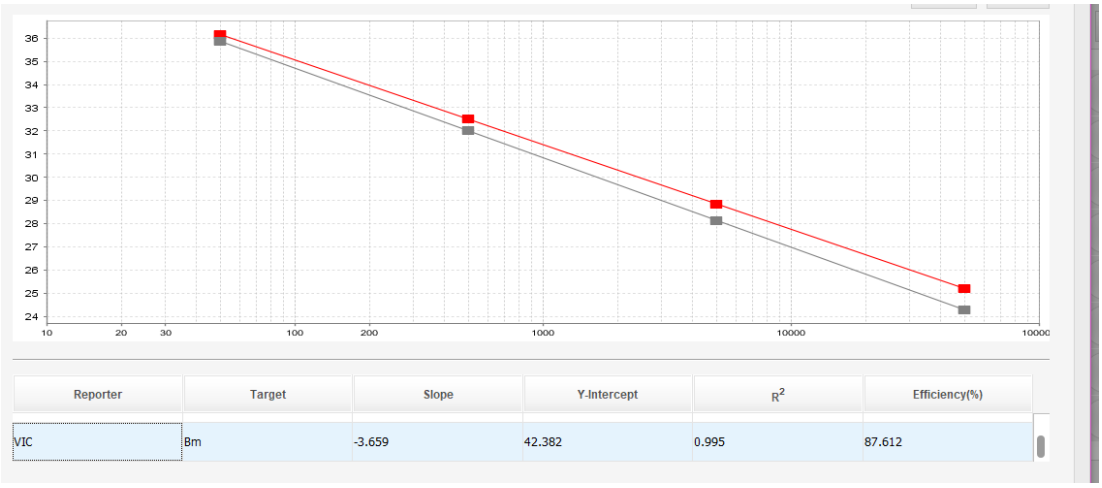

Reporter	Target	Slope	Y-Intercept	R^2	Efficiency(%)
VIC	Bm	-3.659	42.382	0.995	87.612

Figure 39: Standard curve of *B. miyamotoi* serially diluted positive control plasmid DNA with TaqMan probe. The y-axis denotes cycle number and the x-axis denotes copy number. All serial dilution replicates are included.

7.2.2.3 BABESIA MICROTI

The best amplification results of the primers and probe targeting the 18S rRNA gene were obtained at 55°C with 1.00 µM primers and 250 nM probe (Figure 40) with an efficiency of 93.303%. In addition, the standard curve had a R-squared value of 0.965, which supports that the dilutions were accurate (Figure 41). The limit of detection for this set of primers was estimated at 50 copies of the 18S rRNA gene. No troubleshooting was needed for this tick-borne pathogen.

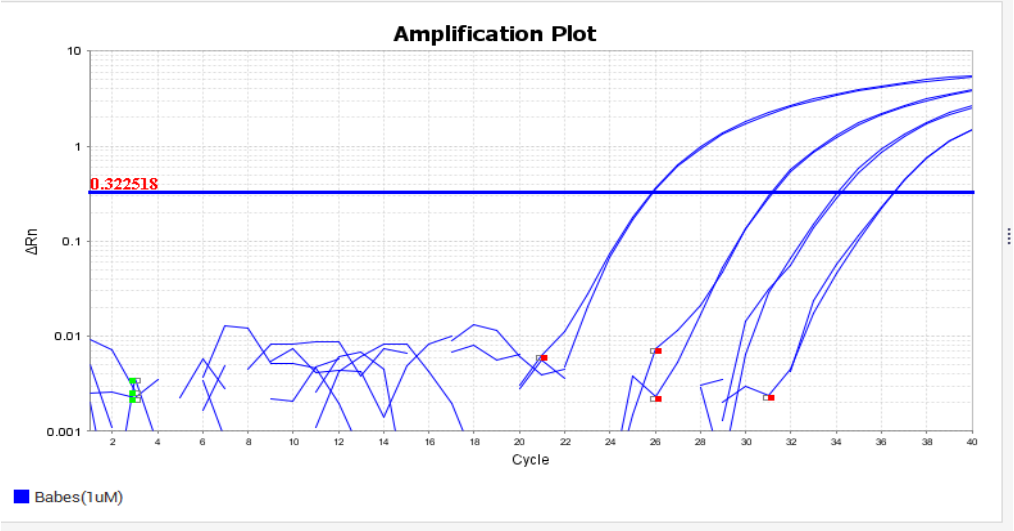

Figure 40: Amplification curve of *B. microti* serially diluted positive control plasmid DNA with TaqMan QSY probe.

Reporter	Target	Slope	Y-Intercept	R^2	Efficiency(%)
FAM	Babes(1uM)	-3.494	42.877	0.965	93.303

Figure 41: Standard curve of *B. microti* serially diluted positive control plasmid DNA with TaqMan probe. The y-axis denotes cycle number and the x-axis denotes copy number. All serial dilution replicates are included.

7.2.2.4 ANAPLASMA PHAGOCYTOPHILUM

Serially diluted positive control plasmid DNA (50,000-50 copies) was combined with varying primer and probe concentrations with the anneal and extend step at 60 °C (Table 25).

Table 25: *A. phagocytophilum* positive control plasmid optimization.

Primer Concentration (µM)	**Probe Concentration (nM)**	**Efficiency (%)**
1.00	250	77.900
0.50	250	83.199
0.25	250	82.071
0.50	300	99.050

The best amplification results of the primers and probe targeting the *msp2* gene (Tables 2 and 4), were obtained with the combination of the 0.50 µM primers and the 300 nM probe with an efficiency of 99.050%, which falls within the acceptable range of amplification. However, due to pipetting error, the standard curve had a R-squared value of 0.953 and the amplification curve was not clean. Therefore, the second-best combination – 0.50 µM primers and the 250 nM probe with an efficiency of 83.199% - was deemed as the better combination (Figure 42). The standard curve had a R-squared value of 0.973, which supports that the dilutions were more accurate than the previous trial (Figure 44). With the omission of one 500 copy replicate, the efficiency increased to 86.025% and the standard curve had a R-squared value of 0.986 (Figure 43). The limit of detection, which was performed with the 250 nM probe, was 50 copies of the *msp2* gene.

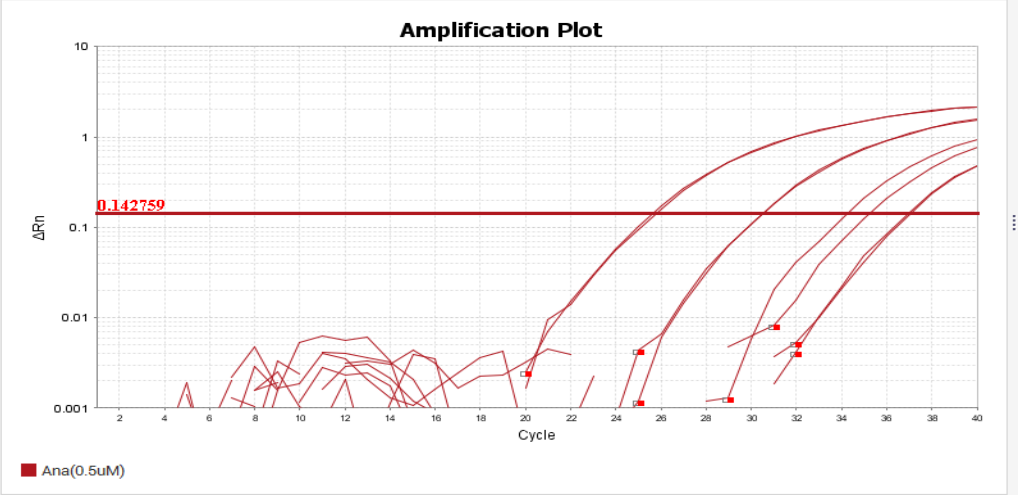

Figure 42: Amplification curve of *A. phagocytophilum* serially diluted positive control plasmid DNA with 250 nM TaqMan QSY probe.

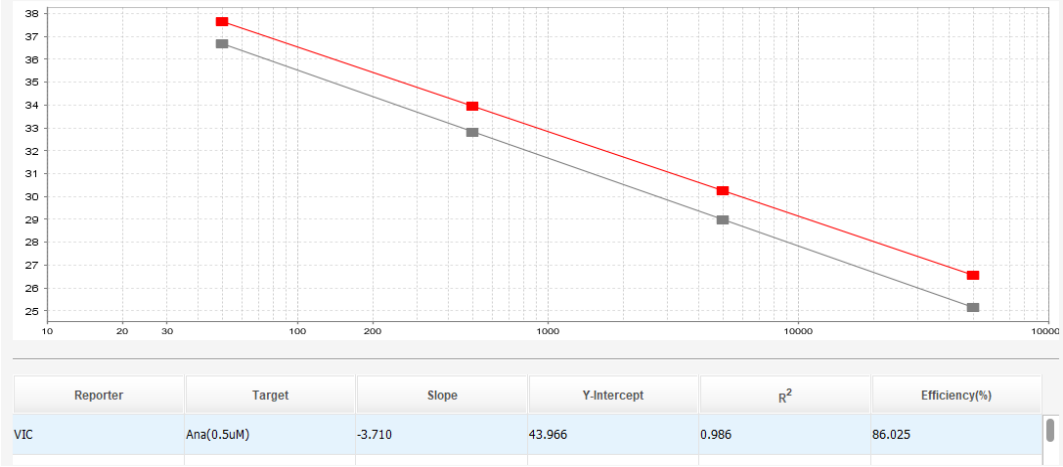

Reporter	Target	Slope	Y-Intercept	R^2	Efficiency(%)
VIC	Ana(0.5uM)	-3.710	43.966	0.986	86.025

Figure 43: Standard curve of *A. phagocytophilum* serially diluted positive control plasmid DNA with 250 nM TaqMan probe. The y-axis denotes cycle number and the x-axis denotes copy number. One 500 copy dilution has been omitted from this analysis.

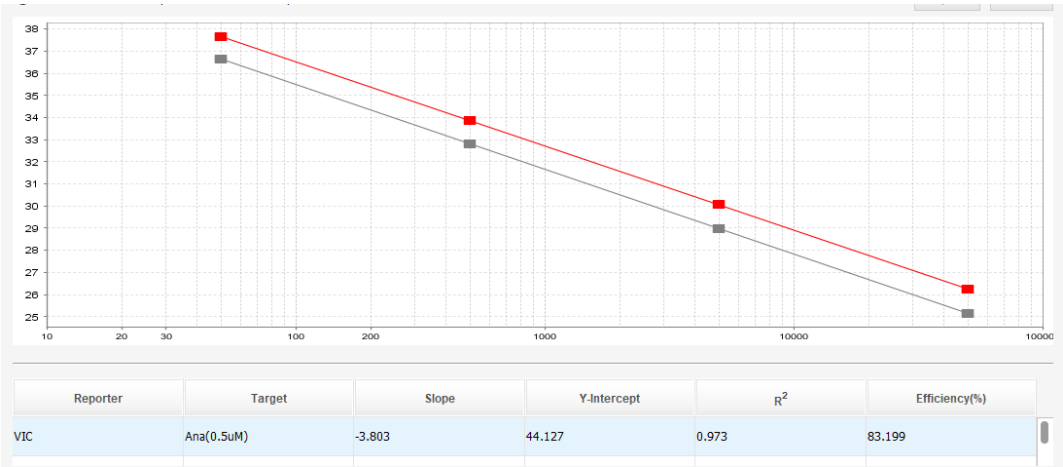

Reporter	Target	Slope	Y-Intercept	R^2	Efficiency(%)
VIC	Ana(0.5uM)	-3.803	44.127	0.973	83.199

Figure 44: Standard curve of *A. phagocytophilum* serially diluted positive control plasmid DNA with 250 nM TaqMan probe. The y-axis denotes cycle number and the x-axis denotes copy number. All serial dilution replicates included.

PART 8 - TAQMAN – FIRST SET OF PRIMERS, SECOND SET OF PROBES WITH CLIENT TICKS

8.1 RESULTS

Client deer ticks were also tested for the presence of the tick-borne pathogens. Three examples of them are provided (Table 26).

Table 26: Client ticks along with their presence or absence of the tick-borne pathogens.

Client Tick	***B. burgdorferi***	***B. miyamotoi***	***B. microti***	***A. phagocytophilum***
ZA			X	
ZB	X	X		X
ZC	X			

X = Positive for that tick-borne pathogen

These ticks were previously tested using the SYBR Green methodology and provided the same results for the tick-borne pathogens as these TaqMan results. Since these trials were successful, if this study is to be continued in the future, more client ticks should be tested with this TaqMan methodology and compared to the SYBR Green methodology before attempting to multiplex the reactions.

8.2 TROUBLESHOOTING

It was important to make sure that when doing the analysis of the standard curves, that the correct fluorescent dye for each probe was properly labeled in the real-time PCR computer program. If the wrong dye was mis-assigned to a PCR well, the real-time PCR

software program analyzed the data incorrectly, which resulted in reaction efficiencies that were inaccurate. To mitigate this issue, careful attention was needed when labeling the PCR well plates.

Additionally, it was important to keep the primers and probes separate from each other as to not have any cross contamination. By making a checklist, we were able to be sure that each PCR reaction had all of its reagents. Finally, since the probes also added one more variable to the reaction mixture, there was much more difficulty in producing efficiencies that were as good as the SYBR reactions. To decrease pipet error, dilutions were made as accurately as possible.

PART 9 - POSITIVE CONTROL PLASMID TRANSFORMATION

9.1 RESULTS

To maintain a stock of positive control for each plasmid, *E. coli* strain DH5**α** was transformed with plasmids pMA-TANA, pMA-TBAB, and pMA-RQMIY as described in material and methods. Growth of the transformed bacteria with the addition of the plasmids was evident (Figures 45-47).

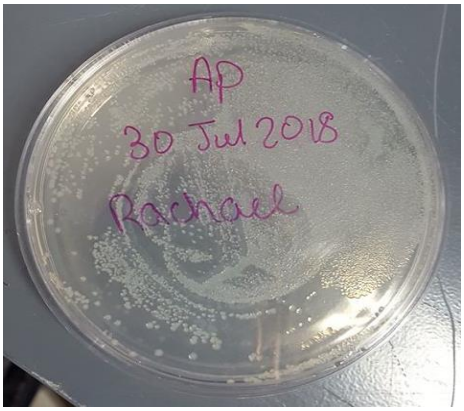

Figure 45: Growth of the transformed *E. coli* cells with the addition of the positive control plasmid for *A. phagocytophilum*.

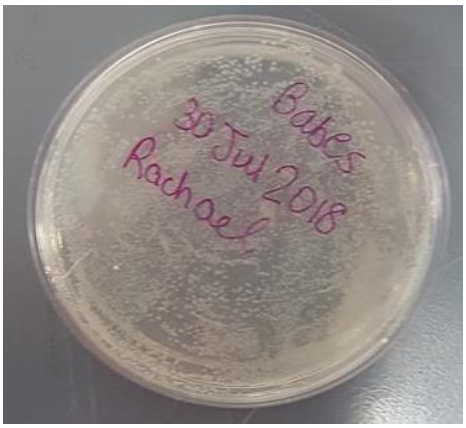

Figure 46: Growth of the transformed *E. coli* cells with the addition of the positive control plasmid for *B. microti*.

Figure 47: Growth of the transformed *E. coli* cells with the addition of the positive control plasmid for *B. miyamotoi*.

After performing the miniprep, the plasmid DNA concentration was read on the Qubit 3.0 and produced the following results (Table 27). Since the first trial (1A-6A) resulted in such poor plasmid yields, a second trial (1B-6B) was conducted with the addition of more LB broth and ampicillin than the previous trial. This allowed more DNA to become pelleted, and thus, resulted in a higher plasmid yield at the conclusion of the miniprep.

Table 27: *B. microti*, *A. phagocytophilum*, and *B. miyamotoi* positive control plasmid transformation DNA yields (ng/µL). OOR = Out of Range

Colony #	***B. microti* Plasmid (ng/µL)**	***A. phagocytophilum* Plasmid (ng/µL)**	***B. miyamotoi* Plasmid (ng/µL)**
1A	Reading 1: 8.92 Reading 2: 11.10 Average: 10.01	Reading 1: 4.60 Reading 2: 4.30 Average: 4.45	Reading 1: 2.24 Reading 2: OOR Average: 2.24
2A	Reading 1: 6.56 Reading 2: 6.70 Average: 6.63	Reading 1: 3.16 Reading 2: 2.86 Average: 3.01	Reading 1: 2.96 Reading 2: 2.68 Average: 2.82
3A	Reading 1: 5.78 Reading 2: 5.72 Average: 5.75	Reading 1: 4.08 Reading 2: 3.74 Average: 3.91	Reading 1: OOR Reading 2: OOR Average: OOR
4A	Reading 1: 2.46 Reading 2: 2.42 Average: 2.44	Reading 1: 2.94 Reading 2: 2.82 Average: 2.88	Reading 1: OOR Reading 2: OOR Average: OOR
5A	Reading 1: 4.26 Reading 2: 3.98 Average: 4.12	Reading 1: 3.08 Reading 2: 3.00 Average: 3.04	Reading 1: OOR Reading 2: OOR Average: OOR
6A	Reading 1: 4.92 Reading 2: 4.72 Average: 4.82	Reading 1: 3.52 Reading 2: 3.32 Average: 3.42	Reading 1: OOR Reading 2: OOR Average: OOR
1B	Reading 1: 47.0	Reading 1: 41.4	Reading 1: 28.2

	Reading 2: 46.0 Average: 46.5	Reading 2: 40.4 Average: 40.9	Reading 2: 27.2 Average: 27.7
2B	Reading 1: 48.2 Reading 2: 48.0 Average: 48.1	Reading 1: 34.4 Reading 2: 34.0 Average: 34.2	Reading 1: 23.8 Reading 2: 23.4 Average: 23.6
3B	Reading 1: 44.8 Reading 2: 45.0 Average: 44.9	Reading 1: 47.4 Reading 2: 45.8 Average: 46.6	Reading 1: 38.6 Reading 2: 37.6 Average: 38.1
4B	Reading 1: 47.0 Reading 2: 46.0 Average: 46.5	Reading 1: 48.4 Reading 2: 47.8 Average: 48.1	Reading 1: 27.4 Reading 2: 26.6 Average: 27.0
5B	Reading 1: 44.6 Reading 2: 43.4 Average: 44.0	Reading 1: 48.4 Reading 2: 47.0 Average: 47.7	Reading 1: 27.2 Reading 2: 26.8 Average: 27.0
6B	Reading 1: NA Reading 2: NA Average: NA	Reading 1: 50.2 Reading 2: 51.4 Average: 50.8	Reading 1: 32.0 Reading 2: 30.8 Average: 31.4

With the transformed plasmid DNA purified and separated from the competent *E. coli*, it was then tested on the quantitative PCR using SYBR Green I and the standardized primers optimized for each of the tick-borne pathogens to be sure that the plasmids were transformed properly. The melt curve part of this experiment was the most important to be sure that the products formed were the correct ones (Figures 48-50).

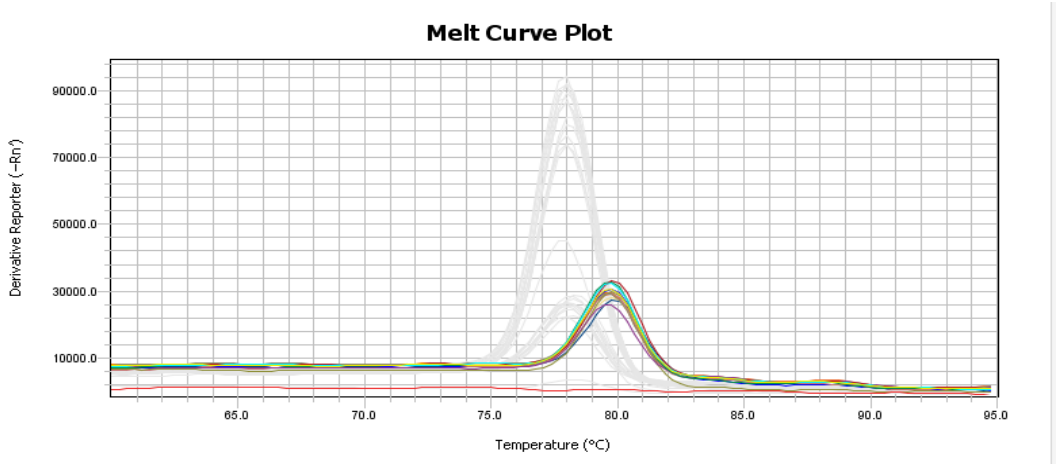

Figure 48: Melt curve of transformed *A. phagocytophilum* positive control plasmid along with the original positive control plasmid stock.

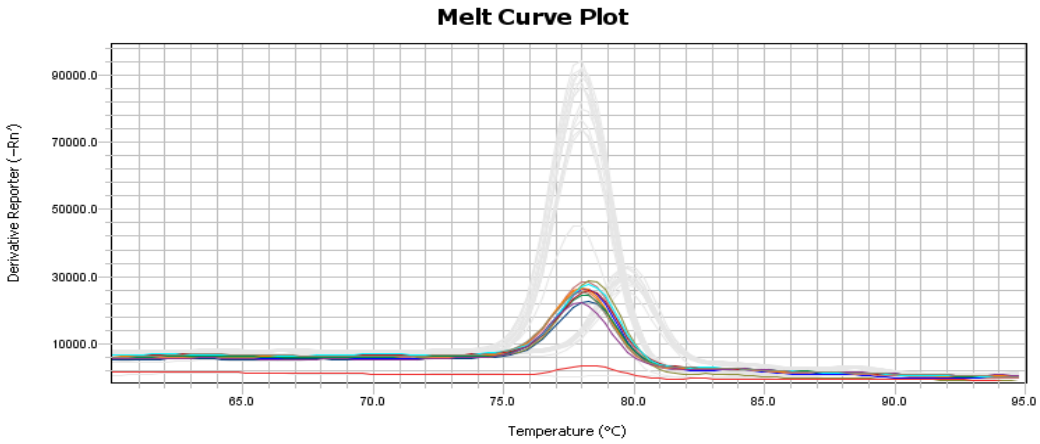

Figure 49: Melt curve of transformed *B. microti* positive control plasmid along with the original positive control plasmid stock.

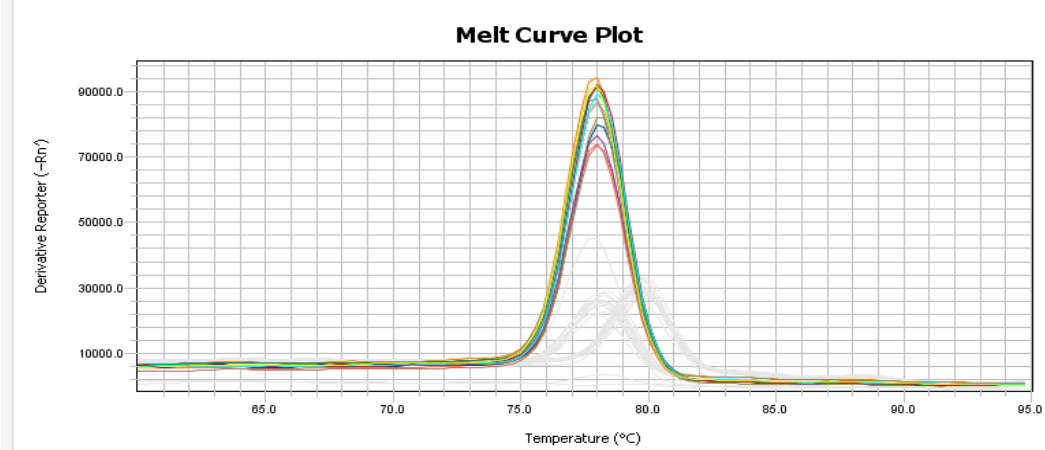

Figure 50: Melt curve of transformed *B. miyamotoi* positive control plasmid along with the original positive control plasmid stock.

9.2 TROUBLESHOOTING

While performing the miniprep of the transformation, only 1.6 mL of the competent *E. coli* with the addition of the plasmid was utilized out of the 3 mL total in each of the Falcon tubes. This caused the plasmid DNA yield to be much lower than expected, below 20 ng/µL, the concentration of the original stock plasmids for *A. phagocytophilum*, *B. microti*, and *B. miyamotoi*. Since the goal of the transformation was to obtain a much higher concentration of plasmid, a larger batch of LB broth with ampicillin was created to allow the *E. coli* to grow in the shaker into a larger quantity. Then during the pelleting step of the miniprep, all of the broth of the *E. coli* with the addition of the plasmid was utilized. This created a larger DNA pellet to carry through the rest of the miniprep, which then resulted in a better plasmid DNA yield.

9.3 COST-BENEFIT ANALYSIS

Each positive control plasmid purchased from Thermo Fisher Scientific was about $550 for 5 micrograms of DNA. From a company standpoint, this can be cost-ineffective for the long term, as it is important to save money wherever possible. By performing the transformation and minipreparation in-house, a plethora of positive control plasmid could be created at a much lower cost. After taking all of the materials needed for the transformation into account (Table 28), the cost per plasmid is $22.18. Additionally, the amount of DNA extracted during the miniprep step exceeded the 20 ng/μL of plasmid DNA bought from Thermo Fisher Scientific and was sometimes even more than double this concentration in a 50 μL aliquot. Therefore, the aliquots could be diluted further to create a larger volume to obtain the same concentration of 20 ng/μL similarly to the $500+ plasmids purchased from Thermo Fisher Scientific. Based on these results, it is more cost effective to make the positive control plasmids through the transformation step versus purchasing them from a separate supplier.

Table 28: Positive control plasmid transformation materials, total cost, and cost per plasmid.

Material	**Total Cost ($)**	**Cost Per Plasmid ($)**
LB Agar, Miller (500 grams)	122.91	0.67
LB Broth, Miller (500 grams)	81.65	0.27
Ampicillin (powdered form, 10 grams)	62.14	0.21
Miniprep Kit Qiagen	92.50	11.10
Competent *E. coli* DH5α (40 reactions)	88.00	6.60
Other Consumables (agar plates, filter, test tubes)	10*	3.33
TOTAL COST PER PLASMID		**$22.18**

* For all three plasmids only. Materials are bought in bulk for other microbiology testing in the laboratory. No materials were purchased separately for the transformation only.

PART 10 - COST BENEFIT ANALYIS, AND TIME SAVED– WHOLE PROJECT

To test a deer tick for all four of its common pathogens using the original gel electrophoresis methodology, each reaction for each individual pathogen needed to be performed in individual PCR tubes. Then, the products from each of the individual reactions have to be run on a gel in order to visualize the presence or absence of the DNA products (72). In theory, this methodology works for a small number of deer ticks. In the

middle of the tick breeding season, though, this was not a time-efficient methodology when twelve or more ticks could be sent in by clients to be tested daily.

By focusing on the time lost in the laboratory (Table 29), the gel setup and run components of the methodology were the time limiting steps. If twelve deer ticks needed to be tested for all four pathogens, five gels with twenty lanes would have been necessary. Between the gel setup and run steps, as well as the PCR amplification step, 23 hours were needed to test all twelve deer ticks. In a normal eight-hour work day, only about two gels could be loaded, ran, and analyzed. This meant that it would take about three days to test all twelve deer ticks for all four of its common pathogens, including the PCR DNA amplification step, as well as the analysis and paperwork to document the findings. Additionally, the large amount of gels meant plenty of lost manhours due to the DNA loading process, as well as the gel setup. During the peak tick breeding season with the laboratory receiving twelve or more ticks a day, it is obvious that this methodology was not efficient, resulting in poor turnaround time of the results to clients and a lack of revenue generated for the company.

Table 29: Gel Electrophoresis hours required for 12 deer ticks.

	DURATION (HOURS)	MANHOURS
PCR SETUP (12 ticks) - 68 rxns	1.5	1.5
PCR RUN (12 ticks)	1.5	0
GEL SETUP	1.5	1
GEL RUN	2	0
GEL ANALYSIS	0.5	0.5
TOTAL	7	3
PCR	3	1.5
Gels (hours * 5)	20	7.5
TOTAL	**23**	**9**

The SYBR Green methodology removed the time-consuming gel electrophoresis setup and run steps, as well as increased the number of ticks able to be tested at one time. To test twelve ticks at one time with the SYBR Green methodology (Table 30), no time was lost during the non-existent gel electrophoresis steps. Even though the PCR component of the process was a bit more time consuming, the amount of manhours was reduced dramatically from nine hours to two hours. In an eight-hour workday, this time saved is huge and extremely beneficial to utilize for other laboratory testing. Additionally, the turnaround time to test twelve ticks went from 23 hours down to three and a half hours with the new SYBR green method. This meant that more than 24 ticks could be tested for all four of its common pathogens each day from start to finish, including the PCR steps, as well as the analysis and paperwork to document findings. This results in more business and revenue for the company with a much more competitive turnaround time as compared to other tick testing businesses.

Table 30: SYBR Green I hours required for 12 deer ticks.

	DURATION (HOURS)	MANHOURS
PCR SETUP (12 ticks) - 68 rxns	1.5	1.5
PCR RUN (12 ticks)	1.5	0
PCR ANALYSIS (12 ticks)	0.5	0.5
GEL SETUP	0	0
GEL RUN	0	0
GEL ANALYSIS	0	0
TOTAL	3.5	2
PCR	3.5	2
Gels	0	0
TOTAL	**3.5**	**2**

With the TaqMan methodology, there are both pros and cons for it being used in a company setting. The largest benefit of using the TaqMan methodology is the ability to test a deer tick for multiple pathogens at the same time in one test tube. Since each probe fluoresces a different colored dye at a different wavelength of light (Figure 51), each pathogen's DNA can be easily differentiated from one to the other (61). The probes allow for greater specificity and do not bind to all forms of double stranded DNA, unlike SYBR Green I. Then, when the DNA is amplified on the quantitative PCR, the amplification curves can not only be seen in real-time, but they are also colored-dye specific. This is an easy way to determine which tick-borne pathogens are present inside of a deer tick or not, without using as many consumables and with a few less steps in the overall methodology. Additionally, this method also saves on the amount of DNA needed from the tick itself. Nymphs and larvae can be tested for all of the tick-borne diseases without the fear of not having enough DNA to work with inside the laboratory.

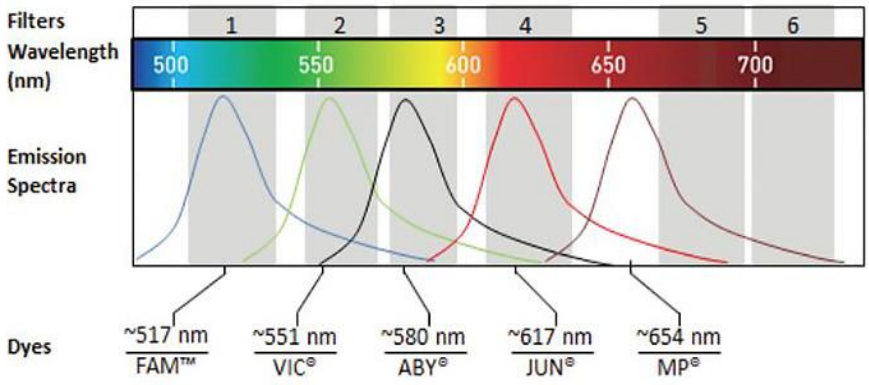

Figure 51: Each TaqMan probe dye along with its wavelength and emission spectra (61).

Even though the TaqMan methodology saves on the number of consumables and has a slightly shorter PCR amplification run-time than the SYBR Green I methodology, it

does not save that much time in the laboratory. More focus is required to be sure all of the primers, tick DNA, and master mix are added into each PCR tube in the correct amounts in preparation of the PCR running, and the analysis takes longer than the normal SYBR green I method to differentiate each tick-borne pathogen. Therefore, it takes more time to test a client's tick this way even with this increase in amplification specificity (Table 31).

Table 31: TaqMan hours required for 20 deer ticks.

	DURATION (HOURS)	MANHOURS
PCR SETUP (20 ticks) - 20 rxns	1.5	1.5
PCR RUN (20 ticks)	1	0
PCR Analysis (20 ticks)	1	1
GEL SETUP	0	0
GEL RUN	0	0
GEL ANALYSIS	0	0
TOTAL	3.5	2.5
PCR	3.5	2.5
Gels	0	0
TOTAL	**3.5**	**2.5**

Also, even though 40 ticks can be tested in one work day with this methodology, it is rare to receive that many ticks from clients in one day even during the busy summer season. Additionally, the TaqMan probes and gene expression master mix are much more expensive, as compared to the cheaper SYBR Green I master mix. With all these factors considered, it is suggested that TaqMan is not the cheapest methodology to utilize in the laboratory, but it does have an increase in specificity with the primers and probes binding to their specific tick-borne pathogen targets.

CONCLUSION

With the conclusion of this project, two efficient methodologies have been created to detect *Anaplasma phagocytophilum*, *Babesia microti*, *Borrelia burgdorferi*, and *Borrelia miyamotoi* in *Ixodes scapularis* using real-time PCR – a SYBR Green methodology and a TaqMan methodology. Both of which are much more efficient and more sensitive than the previous gel electrophoresis methodology. Since the primers and probes are specific to each tick-borne pathogen and have been fully optimized, it is possible to move forward in the future with combining the reactions into one PCR test tube in hopes of creating a TaqMan multiplex PCR methodology.

REFERENCES

1. Chan K, Marras SA, Parveen N. 2013. Sensitive multiplex PCR assay to differentiate Lyme spirochetes and emerging pathogens Anaplasma phagocytophilum and Babesia microti. BMC Microbiology 13:295.
2. Kocan KM, de la Fuente J, Coburn LA. 2015. Insights into the development of Ixodes scapularis: a resource for research on a medically important tick species. Parasites & vectors 8:592-592.
3. Nava S, Venzal JM, González-Acuña D, Martins TF, Guglielmone AA. 2017. Chapter 2 - Genera and Species of Ixodidae, p 25-267. *In* Nava S, Venzal JM, González-Acuña D, Martins TF, Guglielmone AA (ed), Ticks of the Southern Cone of America doi:https://doi.org/10.1016/B978-0-12-811075-1.00002-9. Academic Press.
4. Anonymous. 20 April 2017 2017. Life cycle of Hard Ticks that Spread Disease, *on* Centers for Disease Control and Prevention National Center for Emerging and Zoonotic Infectious Diseases (NCEZID) Division of Vector-Borne Diseases (DVBD). https://www.cdc.gov/ticks/life_cycle_and_hosts.html. Accessed 22 May 2018.
5. Wilson K, Elston D. 2018. What's Eating You? Ixodes Tick and Related Diseases, Part 1: Life Cycle, Local Reactions, and Lyme Disease. Cutis 101:187-190.
6. Richter D, Matuschka F-R, Spielman A, Mahadevan L. How ticks get under your skin: insertion mechanics of the feeding apparatus of Ixodes ricinus ticks. Proceedings Biological sciences 280:20131758-20131758.
7. Yu Z, Wang H, Wang T, Sun W, Yang X, Liu J. 2015. Tick-borne pathogens and the vector potential of ticks in China. Parasites & Vectors 8:24.
8. Moore TC, PµLscher LA, Caddell L, von Fricken ME, Anderson BD, Gonchigoo B, Gray GC. 2018. Evidence for transovarial transmission of tick-borne rickettsiae circulating in Northern Mongolia. PLOS Neglected Tropical Diseases 12:e0006696.
9. Anonymous. 19 January 2018 2018. Geographic distribution of ticks that bite humans, *on* Centers for Disease Control and Prevention National Center for Emerging and Zoonotic Infectious Diseases (NCEZID) Division of Vector-Borne Diseases (DVBD) https://www.cdc.gov/ticks/geographic_distribution.html. Accessed 22 May 2018.
10. Gordon WS, Brownlee A, Wilson DR, Macleod J. 1932. Tick-Borne Fever: A Hitherto Undescribed Disease of Sheep. Journal of Comparative Pathology and Therapeutics 45:301-307.
11. Foggie A. 1951. Studies on the infectious agent of tick-borne fever in sheep. The Journal of Pathology and Bacteriology 63:1-15.
12. Foggie A. 1949. Studies on tick-borne fever in sheep. Journal of General Microbiology.
13. Dumler JS, Choi K-S, Garcia-Garcia JC, Barat NS, Scorpio DG, Garyu JW, Grab DJ, Bakken JS. 2005. Human Granulocytic Anaplasmosis and Anaplasma phagocytophilum. Emerging Infectious Diseases 11:1828-1834.

14. Scorpio DG, Choi K-S, DµMler JS. 2018. Anaplasma phagocytophilum-Related Defects in CD8, NKT, and NK Lymphocyte Cytotoxicity. Frontiers in immunology 9:710-710.
15. Woldehiwet Z. 2010. The natural history of Anaplasma phagocytophilum. Veterinary Parasitology 167:108-122.
16. Dumler JS, Barbet AF, Bekker CP, Dasch GA, Palmer GH, Ray SC, Rikihisa Y, Rurangirwa FR. 2001. Reorganization of genera in the families Rickettsiaceae and Anaplasmataceae in the order Rickettsiales: unification of some species of Ehrlichia with Anaplasma, Cowdria with Ehrlichia and Ehrlichia with Neorickettsia, descriptions of six new species combinations and designation of Ehrlichia equi and & apos; HGE agent & apos; as subjective synonyms of Ehrlichia phagocytophila. International Journal of Systematic and Evolutionary Microbiology 51:2145-2165.
17. Rikihisa Y. 2011. Mechanisms of Obligatory Intracellular Infection with Anaplasma phagocytophilum. Clinical Microbiology Reviews 24:469-489.
18. Biggs HM, Behravesh CB, Bradley KK, Dahlgren FS, Drexler NA, Dumler JS, Folk SM, Kato CY, Lash RR, Levin ML, Massung RF, Nadelman RB, Nicholson WL, Paddock CD, Pritt BS, Traeger MS. 2016. Diagnosis and management of tickborne rickettsial diseases. Recommendations and reports : Morbidity and mortality weekly report Recommendations and reports / Centers for Disease Control 65.
19. Anonymous. 28 June 2018 2018. Anaplasmosis - Epidemiology and Statistics, *on* Centers for Disease Control and Prevention National Center for Emerging and Zoonotic Infectious Diseases (NCEZID) Division of Vector-Borne Diseases (DVBD). https://www.cdc.gov/anaplasmosis/stats/index.html#geography.
20. Western KA, Benson GD, Gleason NN, Healy GR, SchµLtz MG. 1970. Babesiosis in a Massachusetts Resident. New England Journal of Medicine 283:854-856.
21. Spielman A, Clifford CM, Piesman J, Corwin MD. 1979. Human babesiosis on Nantucket Island, USA: description of the vector, Ixodes (Ixodes) dammini, n. sp. (Acarina: Ixodidae). Journal of Medical Entomology 15:218-234.
22. Vannier E, Gewurz BE, Krause PJ. 2008. Human babesiosis. Infectious disease clinics of North America 22:469-ix.
23. Vannier E, Krause PJ. 2012. Human Babesiosis. New England Journal of Medicine 366:2397-2407.
24. Burgdorfer W, Varma MGR. 1967. Trans-Stadial and Transovarial Development of Disease Agents in Arthropods. Annual Review of Entomology 12:347-376.
25. Malaria GHDoPDa. 30 October 2017 2017. Babesiosis, *on* Centers for Disease Control and Prevention. https://www.cdc.gov/dpdx/babesiosis/index.html. Accessed 24 July 2018.
26. SALEH AMA, ADAM SM, ABDEL-MOTAGALY AME-S, MOHAMMAD A, IBRAHIM A, MORSY TA. 2015. HMMAN BABESIOSIS: A GENERAL REVIEW WITH SPECIAL REFERENCE TO EGYPT. Journal of the Egyptian Society of Parasitology 45:493-510.
27. Anonymous. 2009. Etymologia: Babesia [bə-beʹ ze-ə]. Emerging Infectious Disease journal 15:787.

28. Diseases GHDoP. 2014. Babesiosis - Epidemiology & Risk Factors, *on* Centers for Disease Control and Prevention. https://www.cdc.gov/parasites/babesiosis/epi.html. Accessed 24 July 2018.
29. Diseases GHDoP. 17 October 2016 2016. Babesiosis Maps, *on* Centers for Disease Control and Prevention. https://www.cdc.gov/parasites/babesiosis/data-statistics/maps/maps.html. Accessed 24 July 2018.
30. Burgdorfer W, Barbour AG, Hayes SF, Benach JL, Grunwaldt E, Davis JP. 1982. Lyme Disease--A Tick-Borne Spirochetosis? Science 216:1317-1319.
31. Johnson RC, Schmid GP, Hyde FW, Steigerwalt AG, Brenner DJ. 1984. BORRELIA-BURGDORFERI SP-NOV - ETIOLOGIC AGENT OF LYME-DISEASE. International Journal of Systematic Bacteriology 34:496-497.
32. Kumar Singh S, Josef Girschick H. 2004. Molecualar survival strategies of the Lyme disease spirochete Borrelia burgdorferi. The Lancet Infectious Diseases 4:575-583.
33. Steere AC, Broderick TF, Malawista SE. 1978. ERYTHEMA CHRONICMM MIGRANS AND LYME ARTHRITIS: EPIDEMIOLOGIC EVIDENCE FOR A TICK VECTOR1. American Journal of Epidemiology 108:312-321.
34. Barbour AG, Hayes SF. 1986. Biology of Borrelia species. Microbiological Reviews 50:381-400.
35. Tilly K, Rosa PA, Stewart PE. 2008. Biology of Infection with Borrelia burgdorferi. Infectious disease clinics of North America 22:217-234.
36. Hyde JA. 2017. Borrelia burgdorferi Keeps Moving and Carries on: A Review of Borrelial Dissemination and Invasion. Frontiers in Immunology 8.
37. Prevention CfDCa. 4 March 2015 2015. Lyme Disease Transmission, *on* Centers for Disease Control and Prevention National Center for Emerging and Zoonotic Infectious Diseases (NCEZID) Division of Vector-Borne Diseases (DVBD). https://www.cdc.gov/lyme/transmission/index.html. Accessed 13 July 2018.
38. Prevention CfDCa. 13 November 2017. Data and Statistics - Lyme Disease, *on* Centers for Disease Control and Prevention National Center for Emerging and Zoonotic Infectious Diseases (NCEZID) Division of Vector-Borne Diseases (DVBD). https://www.cdc.gov/lyme/stats/index.html. Accessed 13 July 2018.
39. FUKUNAGA M, TAKAHASHI Y, TSURUTA Y, MATSUSHITA O, RALPH D, McCLELLAND M, NAKAO M. 1995. Genetic and Phenotypic Analysis of Borrelia miyamotoi sp. nov., Isolated from the Ixodid Tick Ixodes persulcatus, the Vector for Lyme Disease in Japan. International Journal of Systematic and Evolutionary Microbiology 45:804-810.
40. Kozue S, Ai T, Satoru K, Minoru N, Takuya I, Kojiro K, Minoru K, Makoto O, Hiroki K. 2014. Human Infections with Borrelia miyamotoi, Japan. Emerging Infectious Disease journal 20:1391.
41. Platonov AE, Karan LS, Kolyasnikova NM, Makhneva NA, Toporkova MG, Maleev VV, Fish D, Krause PJ. 2011. Humans infected with relapsing fever spirochete Borrelia miyamotoi, Russia. Emerging infectious diseases 17:1816-1823.
42. Anonymous. 5 June 2018 2018. Borrelia miyamotoi Disease, *on* Centers for Disease Control and Prevention.

https://www.cdc.gov/ticks/tickbornediseases/borrelia-miyamotoi.html. Accessed 23 July 2018.
43. Branda JA, Rosenberg ES. 2013. Borrelia miyamotoi: A lesson in disease discovery. Annals of Internal Medicine 159:61-62.
44. Lopez JE, Krishnavahjala A, Garcia MN, Bermudez S. 2016. Tick-Borne Relapsing Fever Spirochetes in the Americas. Veterinary sciences 3:16.
45. M Shone S, J Dillon H, S Hom S, Delgado N. 2006. A Novel Real-Time PCR Assay for the Speciation of Medically Important Ticks, vol 6.
46. Allerdice MEJ, Pritt BS, Sloan LM, Paddock CD, Karpathy SE. 2016. A real-time PCR assay for detection of the Ehrlichia muris-like agent, a newly recognized pathogen of humans in the upper Midwestern United States. Ticks and tick-borne diseases 7:146-149.
47. Wagner ER, Bremer WG, Rikihisa Y, Ewing SA, Needham GR, Unver A, Wang X, Stich RW. 2004. Development of a p28-based PCR assay for Ehrlichia chaffeensis. Molecular and cellular probes 18:111-116.
48. Hojgaard A, Lukacik G, Piesman J. 2014. Detection of Borrelia burgdorferi, Anaplasma phagocytophilµM and Babesia microti, with two different multiplex PCR assays. Ticks and Tick-borne Diseases 5:349-351.
49. Rejmanek D, Bradburd G, Foley J. 2012. Molecular characterization reveals distinct genospecies of Anaplasma phagocytophilum from diverse North American hosts. Journal of Medical Microbiology 61:204-212.
50. Lin Q, Rikihisa Y, Felek S, Wang X, Massung RF, Woldehiwet Z. 2004. Anaplasma phagocytophilum Has a Functional msp2 Gene That Is Distinct from p44. Infection and Immunity 72:3883-3889.
51. Park J, Choi KS, DµMler JS. 2003. Major surface protein 2 of Anaplasma phagocytophilum facilitates adherence to granulocytes. Infection and immunity 71:4018-4025.
52. Massung RF, Levin ML, Munderloh UG, Silverman DJ, Lynch MJ, Gaywee JK, Kurtti TJ. 2007. Isolation and Propagation of the Ap-Variant 1 Strain of Anaplasma phagocytophilum in a Tick Cell Line. Journal of Clinical Microbiology 45:2138-2143.
53. de la Fuente J, Massung RF, Wong SJ, Chu FK, Lutz H, Meli M, von Loewenich FD, Grzeszczuk A, Torina A, Caracappa S, Mangold AJ, Naranjo V, Stuen S, Kocan KM. 2005. Sequence Analysis of the msp4 Gene of Anaplasma phagocytophilum Strains. Journal of Clinical Microbiology 43:1309-1317.
54. Hanron AE, Billman ZP, Seilie AM, Chang M, Murphy SC. 2017. Detection of Babesia microti parasites by highly sensitive 18S rRNA reverse transcription PCR. Diagnostic Microbiology and Infectious Disease 87:226-228.
55. Kenedy MR, Lenhart TR, Akins DR. 2012. The role of Borrelia burgdorferi outer surface proteins. FEMS immunology and medical microbiology 66:1-19.
56. Cutler SJ, Ruzic-Sabljic E, Potkonjak A. 2017. Emerging borreliae – Expanding beyond Lyme borreliosis. Molecular and Cellular Probes 31:22-27.
57. Schwan TG, Schrumpf ME, Hinnebusch BJ, Anderson DE, Konkel ME. 1996. GlpQ: an antigen for serological discrimination between relapsing fever and Lyme borreliosis. Journal of Clinical Microbiology 34:2483-2492.

58. Bacon RM, Pilgard MA, Johnson BJB, Raffel SJ, Schwan TG. 2004. Glycerophosphodiester Phosphodiesterase Gene (glpQ) of Borrelia lonestari Identified as a Target for Differentiating Borrelia Species Associated with Hard Ticks (Acari:Ixodidae). Journal of Clinical Microbiology 42:2326-2328.
59. Krause PJ, Narasimhan S, Wormser GP, Rollend L, Fikrig E, Lepore T, Barbour A, Fish D. 2013. Human Borrelia miyamotoi Infection in the United States. New England Journal of Medicine 368:291-293.
60. Anonymous. PCR Primer Design Guidelines, *on* Premier Biosoft. http://www.premierbiosoft.com/tech_notes/PCR_Primer_Design.html. Accessed 07 August 2018.
61. Anonymous. 2018. Real-time PCR handbook. ThermoFisher Scientific.
62. Aitken A. 10 Nov 2012 2012. TE buffer (Tris-EDTA buffer), *on* National History Museum. http://www.nhm.ac.uk/content/dam/nhmwww/our-science/dpts-facilities-staff/Coreresearchlabs/te-buffer.pdf. Accessed 05 June 2018.
63. Anonymous. June 2010 2010. Quick Reference Card - AmpliTaq Gold® 360 Master Mix, *on* Applied Biosystems. https://www.thermofisher.com/order/catalog/product/4398881. Accessed 14 August 2018.
64. Anonymous. 04 February 2016. Quick Reference - PowerUp™ SYBR™ Green Master Mix, *on* Thermo Fisher Scientific Inc. Accessed 14 August 2018.
65. Anonymous. 20 July 2016 2016. TaqPath™ ProAmp™ Master Mix - Quick Reference, *on* Thermo Fisher Scientific Inc. Accessed 17 August 2018.
66. Anonymous. July 2010. TaqMan® Gene Expression Master Mix Protocol, *on* Applied Biosystems. Accessed 17 August 2018.
67. Tokarz R, Tagliafierro T, Cucura DM, Rochlin I, Sameroff S, Lipkin WI. 2017. Detection of Anaplasma phagocytophilum, Babesia microti, Borrelia burgdorferi, Borrelia miyamotoi, and Powassan Virus in Ticks by a Multiplex Real-Time Reverse Transcription-PCR Assay. mSphere 2:e00151-17.
68. Varde S, Beckley J, Schwartz I. 1998. Prevalence of tick-borne pathogens in Ixodes scapularis in a rural New Jersey County. Emerging infectious diseases 4:97-99.
69. Jordan RA, Schulze TL, Schulze CJ, Mixson T, Papero M. 2005. Relative Encounter Frequencies and Prevalence of Selected Borrelia, Ehrlichia, and Anaplasma Infections in Amblyomma americanum and Ixodes scapularis (Acari: Ixodidae) Ticks from Central New Jersey. Journal of Medical Entomology 42:450-456.
70. Adelson ME, Rao R-VS, Tilton RC, Cabets K, Eskow E, Fein L, Occi JL, Mordechai E. 2004. Prevalence of Borrelia burgdorferi, Bartonella spp., Babesia microti, and Anaplasma phagocytophila in Ixodes scapularis Ticks Collected in Northern New Jersey. Journal of Clinical Microbiology 42:2799-2801.
71. Schulze TL, Jordan RA, Hung RW, Puelle RS, Markowski D, Chomsky MS. 2003. Prevalence of Borrelia burgdorferi (Spirochaetales: Spirochaetaceae) in Ixodes scapularis (Acari: Ixodidae) Adults in New Jersey, 2000–2001. Journal of Medical Entomology 40:555-558.
72. Koontz L. 2013. Chapter Four - Agarose Gel Electrophoresis, p 35-45. *In* Lorsch J (ed), Methods in Enzymology, vol 529. Academic Press.